

URINE ANALYSIS PLATFORM FOR PATHOGEN SCREENING

A STUDY OF THE DEVELOPMENT OF AN ELECTROCHEMICAL POINT-OF-CARE
URINE ANALYSIS PLATFORM FOR PATHOGEN SCREENING

By LARONA TOTENG, B.Eng.

A Thesis Submitted to the School of Graduate Studies in Partial Fulfilment of the
Requirements for the Degree Master of Applied Science

McMaster University © Copyright by Larona Toteng, April 2019

M.A.Sc. Thesis – L.Toteng

McMaster University – Biomedical Engineering

McMaster University MASTER OF APPLIED SCIENCE (2019) Hamilton, Ontario
(Biomedical Engineering)

TITLE: A study of the development of an electrochemical point-of-care urine analysis
platform for pathogen screening

AUTHOR: Larona Toteng, B.Eng. (McMaster University)

SUPERVISOR: Dr. Leyla Soleymani

NUMBER OF PAGES: 72

Abstract

To reduce the incidence of clinical complications and cost associated with Urinary Tract infections (UTIs), there is a need for the development of a low-cost and culture-free UTI diagnostic test with a rapid sample-to-answer time. The aim of this study is to develop an electrochemical assay for nucleic acid detection that is sensitive and specific. We sought to develop such system by creating an assay that combines low background signals with built-in amplification.

In this work, gold disk macroelectrodes are used in conjunction with a bio-recognition layer to capture pathogen-related nucleic acids and then this event is translated into an electrochemical signal. At first DNA was used as the bio-recognition layer. However, to enhance the system's limit-of-detection (LOD), we developed an assay based on the neutral bio-recognition layer, peptide nucleic acid (PNA). PNA produced a lower background signal compared to DNA and a LOD of 0.001 nanomolar. In order to take advantage of isothermal and low-temperature nucleic acid amplification towards further enhancing the system's LOD, a new assay based on programmable strand displacement coupled with electrochemical readout was employed. The system employed target cycling to produce in-built amplification. With this assay a LOD of 0.5 nM was achieved. Further tuning of probe densities is required to realise lower LODs.

These results illustrate how using PNA produces a lower background signal compared to DNA and that employing a programmable strand displacement assay introduces built amplification into a system. Future studies combining the two systems would be ideally suited for realising an assay that is sensitive and specific.

Acknowledgements

I would like to thank my supervisors, Dr. Leyla Soleymani and Dr Smieja for their guidance over the course of this project.

I would also like to thank our collaborators Dr Li and Alex Wang for providing valuable insights and helping in moving this project forward.

Thank you to the members of Soleymani Lab group for the help and support during this project.

And finally thank you to my friends and family for the immeasurable support they have provided over the years.

Table of Contents

Chapter 1	1
1.1 Urinary tract infections	1
1.2 Biosensors	3
1.3 Electrochemical DNA biosensors	6
1.4 Electrochemical set-up	8
1.5 Electrochemical techniques	9
1.6 Voltammetry techniques	10
1.7 Electrochemical DNA biosensors for UTI detection	13
1.8 Objective of thesis	15
Chapter 2	16
2.1 Introduction	16
2.2 Results and discussion	16
2.2.1 Implementation of in-solution reporter system using DNA probes	17
2.2.2 Implementation of in solution reporter system using PNA probes	21
2.3 Conclusion	26
2.4 Experimental Section	26
Chapter 3	30
3.1 Introduction	30
3.2 Results and discussion	31
3.3 Conclusion	46
3.4 Experimental Section	47
Chapter 4	50
4.1 Thesis Findings and Contributions	50
4.2 Future Work	52
Chapter 5 Bibliography	54

List of Figures

Figure 1.1. Key elements of a biosensor	4
Figure 1.2. General working principle of a DNA electrochemical biosensor	7
Figure 1.3. Traditional set-up of an electrochemical biosensor.	8
Figure 1.4. Types of voltammetry scans.....	12
Figure 1.5. Schematic of electrochemical UTI biosensor in the UtiMax™	13
Figure 2.1. Sketch Map of Electrochemical DNA Sensing Strategy employing DNA probes.	19
Figure 2.2. Characterisation of the modified electrode surface	21
Figure 2.3. Sketch Map of Electrochemical DNA Sensing Strategy employing PNA probes	23
Figure 2.4. Detection limit of PNA assay.....	24
Figure 3.1 Sketch Map of strand displacement assay.....	33
Figure 3.2. Characterisation of the modified electrode surface	36
Figure 3.3. Optimisation of concentration of intermediates L1T1RP	38
Figure 3.4. a) Schematic representation of full assay.....	40
Figure 3.5. SWV responses of assay to different concentrations of target DNA	41
Figure 3.6 Grubbs outlier test for peak cathodic and anodic FOCN CV currents for all 24 electrodes used in the two LOD experiments.....	43
Figure 3.7 Characterisation of the oligonucleotides involved in the assay..	45

List of Abbreviations

antimicrobial susceptibility test: AST

Counter electrode : CE

Cyclic voltammetry: CV

Differential pulse voltammetry:DPV

Electrochemical impedance spectroscopy:EIS

FiCN:[Fe(CN)₆]³⁻

FoCN:Fe(CN)₆⁴⁻

horseradish peroxidase:HRP

leukocyte esterase:LE

limit of detection:LOD

Reference electrode:RE

RuHex:[Ru(NH₃)₆]³⁺

Square wave voltammetry:SWV

Urinary tract infections:UTIs

Urine Culture:UC

White blood cells:WBCs

Working electrode:WE

Declaration of Authorship

I, Larona Toteng, hereby declare that I am the sole author of this thesis titled, “A study of the development of an electrochemical point-of-care urine analysis platform for pathogen screening”. This is a true copy of the thesis, including any required final revisions, as accepted by my examiners.

I understand that my thesis may be made electronically available to the public.

Chapter 1

INTRODUCTION

1.1 Urinary tract infections

Urinary tract infections (UTIs) occur when a microbial pathogen is present in the urinary tract. They are typically categorised according to the site of infection, whether they are “complicated” or “uncomplicated”, and finally if they are symptomatic or asymptomatic. Bacteriuria, cystitis and pyelonephritis refer to an infection located in the urine, bladder and kidney respectively. UTIs that occur in a normal genitourinary tract with no history of instrumentation are referred to as uncomplicated while those that occur in genitourinary tracts with abnormalities or a history of instrumentation such as indwelling catheters are referred to as complicated[1].

Testing for UTIs usually starts with dipstick urinalysis. Dipsticks are quick, inexpensive and readily available for physician office use [2][3][4]. The prevailing type of dipstick measures levels of the leukocyte esterase (LE), nitrite and red blood cells. LE is an enzyme that is produced by white blood cells (WBCs), which are increased in urine at the time of infection. Nitrites are produced by some bacteria that release enzymes that convert nitrates to nitrites. Presence of red blood cells in urine may be due to a different pathology, but if they are present along with nitrites and LE, then there is an increased probability of a UTI. Dipsticks are positive for $>5-15$ WBC/high-power field for LE, $>10^5$ cfu/ml for nitrites, and $>1-4$ red blood cells/high power field for red blood cells[2]. Although

dipsticks are quick and convenient, various previous studies have advised that they are not sufficiently sensitive to identify infection[5][6][7].

Dipstick urinalysis is usually performed in conjunction with urine culture (UC). UC is considered the gold standard for UTI diagnosis and is the most common type of culture in many clinical laboratories [5][8][9][10]. It usually involves inoculation of urine on solid agar media and incubation at 35-37 °C overnight. This is followed by pathogen identification and antimicrobial susceptibility testing[8]. The standard threshold for bacteriuria is $>10^5$ cfu/ml, although this threshold has a high false negative rate (50-70 % sensitivity). Previous studies have shown that 30-50 % of women with symptomatic UTIs can have culture amounts as low as 10^2 cfu/ml [2]. Although UCs are great for pathogen identification and performing sensitivity tests, they are also time intensive, labor intensive and also require skilled personnel[8][11]. The total time from urine collection to pathogen identification is generally 18-30 hours. For tailored infection-specific antibiotic treatment to be administered, antimicrobial susceptibility testing (AST) must occur. This increases the total wait time for analysis to 48 hrs [12]. Matrix Assisted Laser Desorption/Ionization-Time of Flight (MALDI-TOF) can be used to lessen the time to pathogen identification to less than 5 hours and it only costs per sample half that of culture. But the initial price purchase of these instruments is over \$250 000 potentially restricting their use to high volume laboratories only [12].

The accurate diagnosis of UTIs usually requires both the presence of symptoms and a positive urine culture[2][4][13]. As such it can be challenging to diagnose UTIs as they present differently in different subgroup and regularly used testing methods can additionally complicate the diagnosis[2]. A study by Mclsaac *et al.*[14] found that even

with the most sensitive measure for urine culture of $>10^2$ cfu/ml, a diagnostic algorithm that encompassed urinary symptoms and a positive dipstick test had a sensitivity of 80.3 % and a specificity of 53.7 %. A review by Schmiemann *et al.*[4] found that various diagnostic algorithms that included both urinary symptoms and positive dipstick tests had an extensively varied sensitivity and specificity (65-82 % and 53-95 % respectively).

Professional recommendations for diagnosis of UTI for women are that those that present with symptoms of acute cystitis receive empirical antibiotic treatment[15]. However, a study by McIssac *et al.*[16], which sought to discover the effect of empirical management of acute UTI on unnecessary antibiotic use, found that of the 186 patients prescribed antibiotics, 74 (39.4 %) were culture negative. The study involved a sample size of 231 women and the prevalence of UTI in this population was 53.3 %. Empirical antibiotic treatment has contributed to the rise in the prevalence of antibiotic resistance in uropathogens [2] [11][17][18][19] [20].

As shown, it can be difficult to accurately diagnose UTIs and this has led to huge societal costs. With roughly 150-250 million cases worldwide, UTIs are one of the most prevalent types of communicable diseases [21][22]. They are a large contributor to medical related expenses and in the US alone they are estimated to have an overall societal cost of around US\$3.5 billion annually[21]. This work will present a study to develop a low-cost and culture-free UTI diagnostic test with rapid sample-to-answer time that is sensitive and specific.

1.2 Biosensors

International Union of Pure and Applied Chemistry (IUPAC) defines biosensors as “a self-contained integrated device which is capable of providing specific quantitative or semi-quantitative analytical information using a biological recognition element which is in direct spatial contact with a transducer”[23]. There are three key parts to a biosensor(Figure 1.1)[24]: a) the sensing element, which is biologically derived; b) the transducer, which converts the sensed signal into a readable and quantifiable output and c) the signal processor which displays the converted signal in an accessible way.

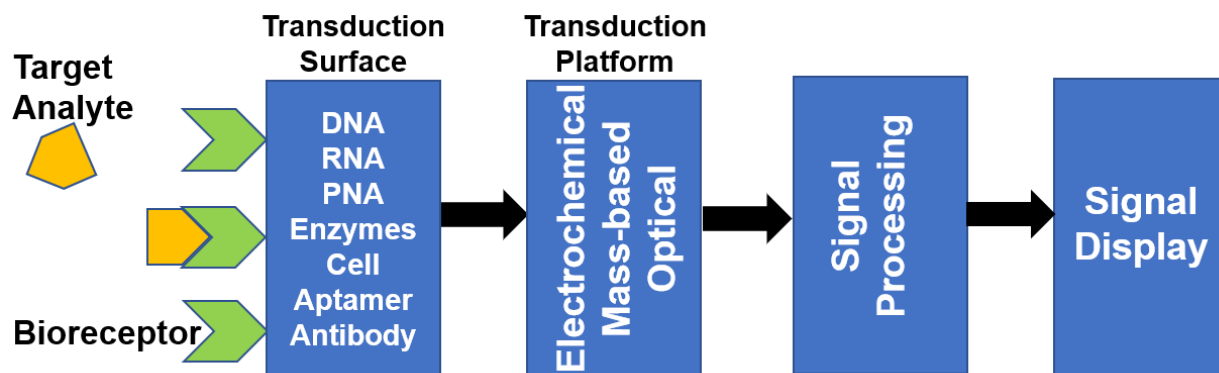


Figure 1.1. Key elements of a biosensor: the sensing element composed of bioreceptors, the transducer, the signal processor and the display.

Biosensors may be classified according to the type of sensing/bio-recognition element used or according to the type of signal transduction platform used.

Biorecognition elements may be broadly classified into two kinds: biocatalytic recognition element or bio-affinity recognition element. In biocatalytic sensors, the interaction between target analytes and bioreceptors is not permanent. The bioreceptor catalyzes a reaction involving the target analyte. Examples of biocatalysts include enzymes, whole

cells, tissue and catalytically active polynucleotides (DNAzymes). In bio-affinity sensors, there is permanent or semi-permanent binding between target analytes and bioreceptors. Examples of bio-affinity include antibody-antigen (immunosensors) interactions, probe and complementary nucleic acid target binding (nucleic acid biosensor), and synthetic oligonucleotides that selectively bind to ligands (aptamer biosensing). [23][25]

Signal transduction platforms may be broadly separated into three categories: electrochemical, mass-based and optical. Electrochemical transducers make use of the oxidation-reduction capability of an electroactive substance in solution. The target analyte may itself be electroactive, or an electroactive tag may be adhered to the analyte, an electroactive species may also be produced from the catalytic breakdown of the target analyte. In electrochemical sensors, there is a production or consumption of ions/electrons from before to after the target analyte binds to the bioreceptor. Mass-based transducers are most generally of the piezoelectric variety. Piezoelectric materials translate mechanical energy into electric energy and conversely electric into mechanical energy. In these sensors, usually a change in resonant frequency occurs from before to after target analyte binds to bioreceptor. Optical transducers usually involve the binding of an optically active substrate to the target analyte, or the catalytic production of an optically active substrate. In this type of sensor there is a change in optical properties from before to after the target analyte binds to the bioreceptor.[25]

Electrochemical biosensors have attracted great attention in research due to their intrinsic advantage of having maintained a close association with advances in the low-cost manufacture of microelectronics. This means electrochemical sensing circuits would be easier to combine with standard electronic read-out and processing than other kinds of

sensors. Other advantages include robustness, ease of miniaturization, low sample volume requirement and low limits of detection. [26]

This diagnostic test that will be explored in this study is an electrochemical DNA biosensor.

1.3 Electrochemical DNA biosensors

Ever since the discovery of the double helix assembly of DNA in 1953 [27], there has been great interest in classifying and sequencing DNA molecules. Any nucleic-acid that is specific to a pathogen can provide an effective way to detect and diagnose an infectious disease. The foundation of all DNA sensors is the ability of a specific DNA sequence to hybridize with its complementary strand. In electrochemical detection of DNA, a current response, under a regulated potential, is generated in response to the hybridization event. The current response is typically due to a change in an electroactive reporter, but it may also be due to other deviations to electrochemical parameters such as resistivity or conductivity. In developing a DNA biosensor, the fabrication of an efficient DNA probe-modified electrode and the design of said DNA probe is immensely important.[28]

The working principle of electrochemical DNA biosensors is summarized in Fig 1.2. An electrode is modified, usually using DNA probes. The electrode is incubated with solution containing target DNA. When target DNA hybridizes with probe DNA, a current response is generated. Stability of probes, hybridization efficiency and minimization of non-specific adsorption all play a vital role in the performance of the biosensor.

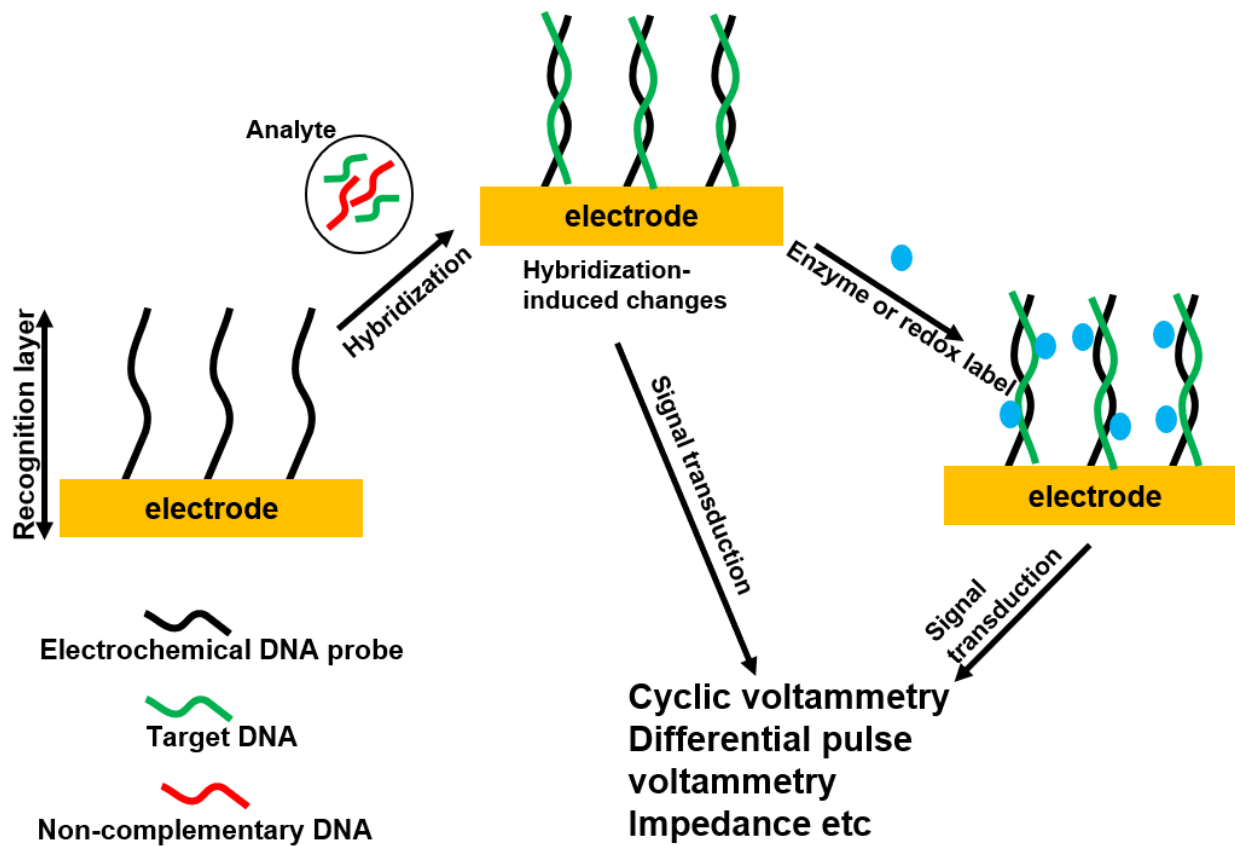


Figure 1.2. General working principle of a DNA electrochemical biosensor. Adapted from [28].

1.4 Electrochemical set-up

Electrochemical events are often monitored using a cell made up of three electrodes (Fig 1.3): a working electrode (WE) where the hybridisation-induced change in an electroactive reporter occurs and is measured, the counter electrode (CE) which equilibrates the current and completes the circuit that makes up the cell, and the reference electrode (RE) that sets the potential at the WE.

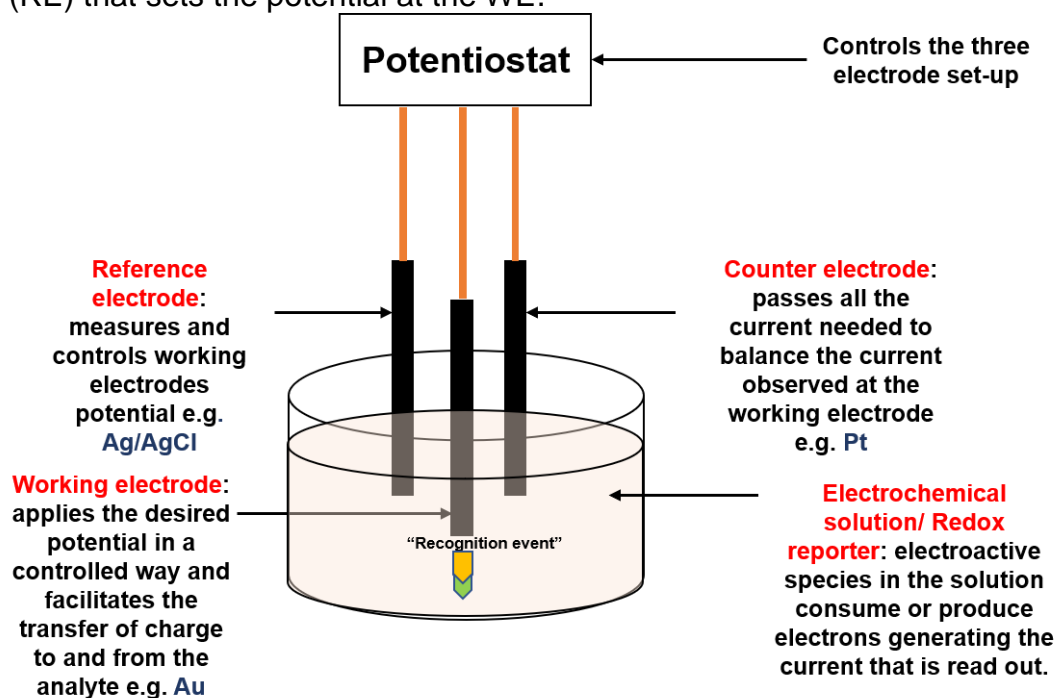


Figure 1.3. Traditional set-up of an electrochemical biosensor.

The WE and CE are usually in direct contact with an analyte solution, while the RE is typically in indirect contact via a salt bridge. When a WE with excess charge on its surface is in direct contact with a solution, an electrical double-layer of ions is formed at the surface. The inner layer is closest to the WE surface, and it comprises of ions in solution that are oppositely charged from the excess charge on the WE surface. The outer layer is referred to as the diffuse layer, and it comprises of ions that are oppositely charged to

the ions in the inner layer. The concentration of the ions in the diffuse layer decreases exponentially the further away you move from the inner layer. Electroactive species move from the bulk solution to the double layer through one of three modes: diffusion down the electroactive species' diffusion gradient from bulk solution to double layer, migration due to the potential gradient between the bulk solution and WE surface, and convection due to a mechanical force like shaking.[25]

1.5 Electrochemical techniques

The three commonly used electrochemical techniques for biosensing are amperometry, voltammetry and electrochemical impedance spectroscopy (EIS). Amperometry involves measuring the time varying current generated by an electrochemical reaction while the potential between the WE and CE is kept constant. For a system with no migration or convection forces at play, the time dependence of the current generated can be related back to the concentration of electroactive species in solution. Voltammetry involves applying a time varying potential between the WE and CE electrodes and measuring the current generated. The types of voltammetry techniques used in this work will be further elaborated upon in the next section. In EIS, a small sinusoidal AC potential superimposed onto a DC potential is applied between the WE and RE, and the resulting phase angle and magnitude of the current generated is measured as a function of the AC frequency. For analysis, the complex current is converted to impedance, and at low frequencies the impedance comprises of only the real (resistive) part. This resistance is termed the charge transfer resistance and can be related to the electroactive analyte concentration. At medium frequencies, the capacitive component of the impedance is related to the

capacitance of the electric double layer. EIS can therefore be used to characterise the performance of a functionalized electrode surface by analysing the resistive and capacitive components of such surfaces. [25]

1.6 Voltammetry techniques

The voltammetry techniques applied in this work are cyclic voltammetry (CV), differential pulse voltammetry (DPV) and square wave voltammetry (SWV).

In CV, the potential (E) between WE and CE is linearly swept (with a scan rate, ν) from an initial value to an end value that when reached the direction of the scan is reversed (Fig 1.4 a). In Fig. 1.4 a) (right) when the potential becomes more positive, the electroactive analyte being interrogated becomes oxidised, when the potential becomes more negative, the analyte is reduced. This is a reversible system, each oxidation and reduction sweep has an associated peak current, i_{pa} and i_{pc} respectively.[29] A peak current i_p is associated with the scan rate ν by the Randles-Sevcik equation:

$$i_p = (2.69 \times 10^5) ACD^{(1/2)}n^{(3/2)} \nu^{(1/2)} \quad (1)$$

Where A = electrode area, C = concentration of analyte, D = diffusion coefficient of analyte, and n = number of electrons transferred from/to analyte in each reaction. For a reversible system the difference between peak potentials is:

$$E_{p-p} = |E_{pa} - E_{pc}| = 59 \text{ mV}/n \quad (2)$$

The further away from reversibility a system is, the less it fits the above equation.

In DPV, the potential waveform applied between WE and CE is a pulse of constant amplitude superimposed over a staircase waveform (Fig 1.4 b). It is used to reduce the

charging current brought about by the electrical double layer. The double layer that forms in proximity to a charged WE in an analyte solution acts similar to a parallel plate capacitor. It produces a non-faradaic (not caused by redox active analyte) current when a potential is applied across the it. DPV reduces this charging current by taking two measurements, one just before the pulse at time τ and one at a time τ_1 late in the pulse, and plotting the current difference ($I_{\tau_1} - I_{\tau}$) against baseline potential. As charging current decays much faster than faradaic current, subtracting the later current from the current just before the pulse reduces the contribution of the charging current and leads to a more precise measurement for the concentration of analyte. This makes DPV more sensitive than CV in detecting lower concentrations of analytes.[30]

In SWV, the potential waveform applied between WE and CE is a square wave superimposed over a staircase waveform (Fig 1.4 c). As with DPV the current is sampled twice, but in this case, it is during the end of a forward pulse and again at the end of a reverse pulse. If the forward pulse oxidizes the electroactive species, the reverse pulse reduces it. The difference of the forward current from the reverse current is plotted against the corresponding staircase tread potential. As currents are sampled at the end of a pulse, the effect of charging currents is minimized just as with DPV. The advantage of SWV over DPV is that since a reverse pulse is applied there is no need to wait for equilibrium condition to be established before the next forward pulse. This means SWV is much faster than DPV analysis and can take seconds for a scan that would take minutes in DPV.[29]

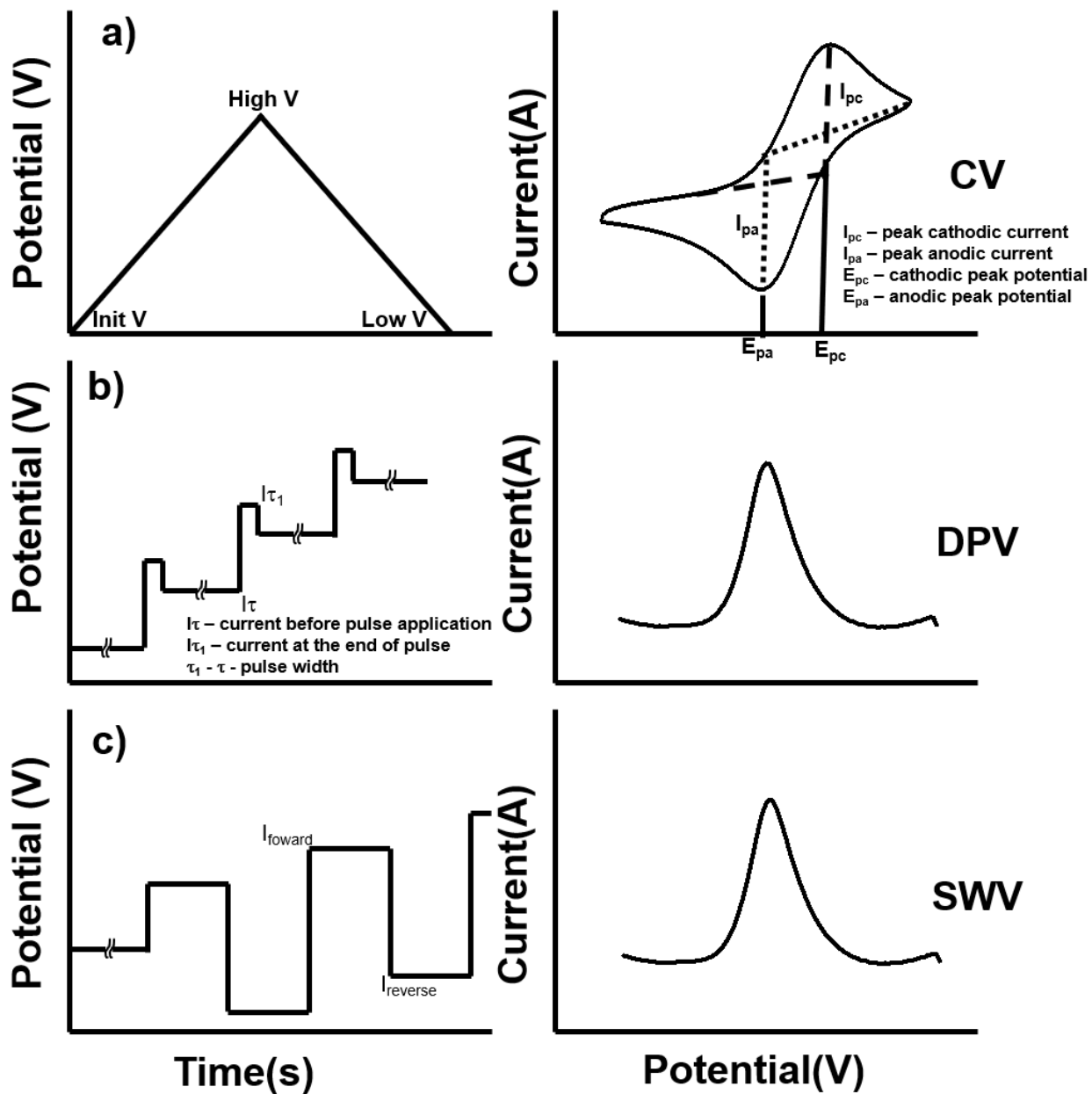


Figure 1.4. (Left) The applied waveform for a) cyclic voltammetry b) differential pulse voltammetry c) square wave voltammetry. (Right) The resulting current waveforms for a reversible redox reaction for each technique.

1.7 Electrochemical DNA biosensors for UTI detection

There are many emerging technologies for rapid and sensitive UTI detection, from image based to molecular and biochemical based technologies, and a full summary of these is presented by Maugeri *et al.*[11]. Since this work employs electrochemical methods, this section will focus on reviewing the only emerging DNA electrochemical sensor for UTI detection that was found by this author to be clinically approved (CE approved).

UtiMax™ is an electrochemical UTI detection technology by GeneFluidics. The method employed in the device involves the electrochemical measurement of bacterial 16S rRNA. 16S rRNA bound to 21 proteins forms the smaller subunit of prokaryotic ribosomes. In cells, ribosomes are implicated in protein synthesis. 16S rRNA is vastly conserved

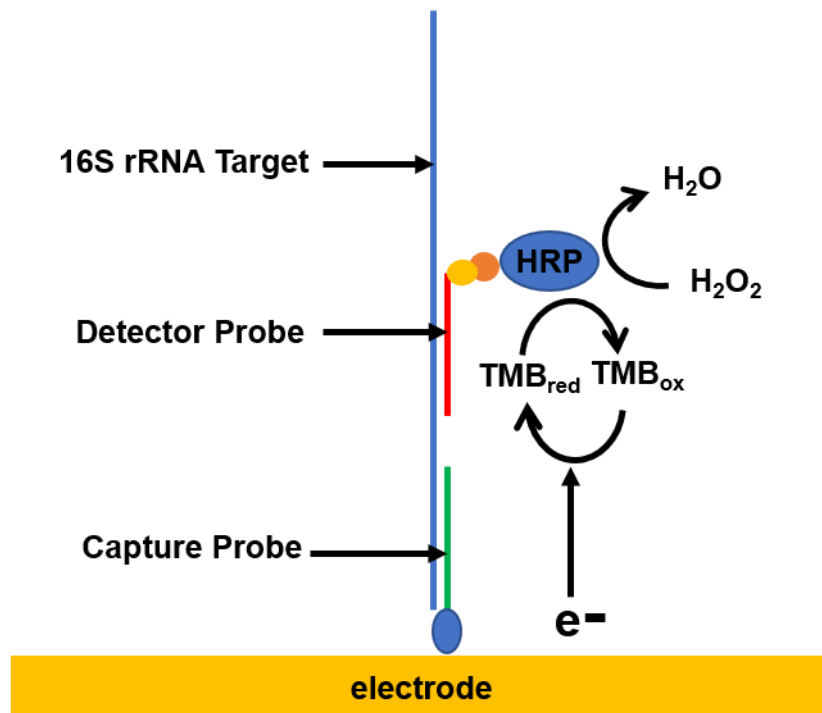


Figure 1.5. Schematic of electrochemical UTI biosensor in the UtiMax™. Adapted from [32].

between bacterial species and is used in bacterial identification[31].

In this assay (Fig 1.5), bacterial samples are first lysed to release the target 16S rRNA. The target strand then binds to the fluorescein tagged detector probe. The detector probe and target duplex then bind to a capture probe on a gold working electrode (WE). The WE is then incubated with anti-fluorescein-conjugated horseradish peroxidase (HRP) reporter enzyme. The substrate 3,3',5'-tetramethylbenzidine (TMB)-H₂O₂ solution is then introduced onto the electrode. A fixed potential of -200 mV is applied to the WE and the amperometric current versus time generated is measured after the HRP redox reaction reaches steady state (60 seconds). The sensor chip consists of an array of sensors which are functionalized with probes for the following species: *Escherichia coli*, *Pseudomonas aeruginosa*, *Klebsiella oxytoca*, *Klebsiella pneumoniae*, *Citrobacter freundii*, *Enterobacter aerogenes*, *Enterobacter cloacae*, *Morganella morganii*, *Serratia marcescens*, *Proteus mirabilis*. Additional sensor array on the chip consist of an AST panel for: Gentamicin, ciprofloxacin, cefepime, trimethoprim/sulfamethoxazole, ceftriaxone, nitrofurantoin and meropenem. Pathogen identification occurs directly on urine patient samples and AST occurs after 3 hours of culture. The whole procedure from pathogen identification to AST is less than four hours. Clinical validation studies for this device have obtained sensitivity of 97 %, specificity of 89 % and limit of detection of 10⁴ cfu/ml, which depending on the species of bacteria, translates to a molar concentration of 2-20 pM (the concentration of ribosomes depending on species, growth stage and time of lysis varies between 7,000 – 70 000 copies). [12] [32][33][34][35][36]. The assay described here is enzymatic, and one big disadvantage to enzymatic biosensor is their sensitivity to their environment. Enzyme activity varies with even the smallest change to their environment [37]. Chemical

instability and sensitivity are a major hurdle to overcome with these kinds of assays and this makes it more difficult to translate them into point-of-care diagnostics. [38]

1.8 Objective of thesis

The primary objective of this thesis is to explore the development of an enzyme and culture free electrochemical point-of-care urine analysis platform for pathogen screening. The main pathogen of interest will be *E.coli* as it causes around 75 % community-acquired UTIs and around 50 %-65 % hospital acquired infections[39].

Chapter 2

2.1 Introduction

With roughly 150-250 million cases worldwide, urinary tract infections (UTIs) are one of the most prevalent types of communicable diseases [21][22]. UTIs are a large contributor to medical related expenses and in the US alone they are estimated to have an overall societal cost of around US\$3.5 billion annually[21]. Due to their high level of incidence, UTIs are one of the main promoters to antibiotic use and hence resistance[40]. To reduce the prevalence of such clinical complications and their associated cost, there is a need for the development of a low-cost and culture-free UTI diagnostic test with an accelerated sample-to-answer time. Electrochemical DNA biosensors have emerged as one of the more attractive avenues for point-of-care (POC) DNA sensing due to their high sensitivity and ease of adaptability into portable, low cost devices[41].

In this chapter, we present a study to develop a rapid electrochemical sensor for nucleic acid detection of UTIs that is sensitive and specific. To achieve this goal, we first introduce a system whereby DNA probes are used as a bio-recognition layer for the sensor. As this system produces high background signals, we demonstrate how switching to the neutral bio-recognition layer peptide nucleic acid (PNA), produces lower background signals leading to lower limits of detection.

2.2 Results and discussion

2.2.1 Implementation of in-solution reporter system using DNA probes

In order to develop a rapid electrochemical assay for nucleic acid detection of UTIs, we first employed an assay whereby the reporter system was in solution. This system consisted of redox active $[\text{Ru}(\text{NH}_3)_6]^{3+}$, (RuHex) and $[\text{Fe}(\text{CN})_6]^{3-}$ (FiCN) and was first employed by [42]. In this system, the positively charged RuHex complex is attracted to and electrostatically binds to the negatively charged phosphate DNA backbone. When a negative potential is applied to the gold working electrode the RuHex ion is reduced, while the negatively charged FiCN complex ion is electrostatically repelled from the electrode surface. As it is much easier to reduce the FiCN ion [43], it is chemically reduced by the RuHex. This oxidises RuHex and regenerates it to again be reduced by the applied potential. It is in this manner that the signal from the RuHex is amplified. In this assay, we immobilised DNA probes onto a gold electrode surface, backfilled the electrode surface with MCH to prevent non-specific adsorption and then introduced a target sequence complementary to the probe DNA (Fig 2.1). This target sequence is a short 20 bases oligonucleotide sequence which is analogous to a section of mRNA in a strain of *E. coli* [44] as *E. coli* is the most frequent cause of UTIs [45]. Target strands were introduced to sensor surface in buffer solutions of 25 mM NaCl, 25 mM PB and 100 mM MgCl_2 . Experiments were carried out in buffer in order to maximise signals under ideal conditions. This is in the hope that when actual urine samples are used, the inevitable dampening of the signal is not so great as to lead to total loss of signals.

We characterised the electrode surface by running cyclic voltammetry scans in 2 mM $\text{Fe}(\text{CN})_6^{4-}$ (FoCN) solution (Figure 2.2 a). When the electrode surface is bare, the negatively charged FoCN ions can approach the electrode surface, such that when a

potential is applied, the FoCN ions are oxidised and a current is generated. After deposition of the probe DNA, there are more negative charges on the electrode surface, leading to the FoCN ions to be repelled and less oxidation to occur, hence less current is generated. When target strands are introduced, the amount of negative charges at the electrode surface is increased, hence more repulsion, less oxidation and even less current generation.

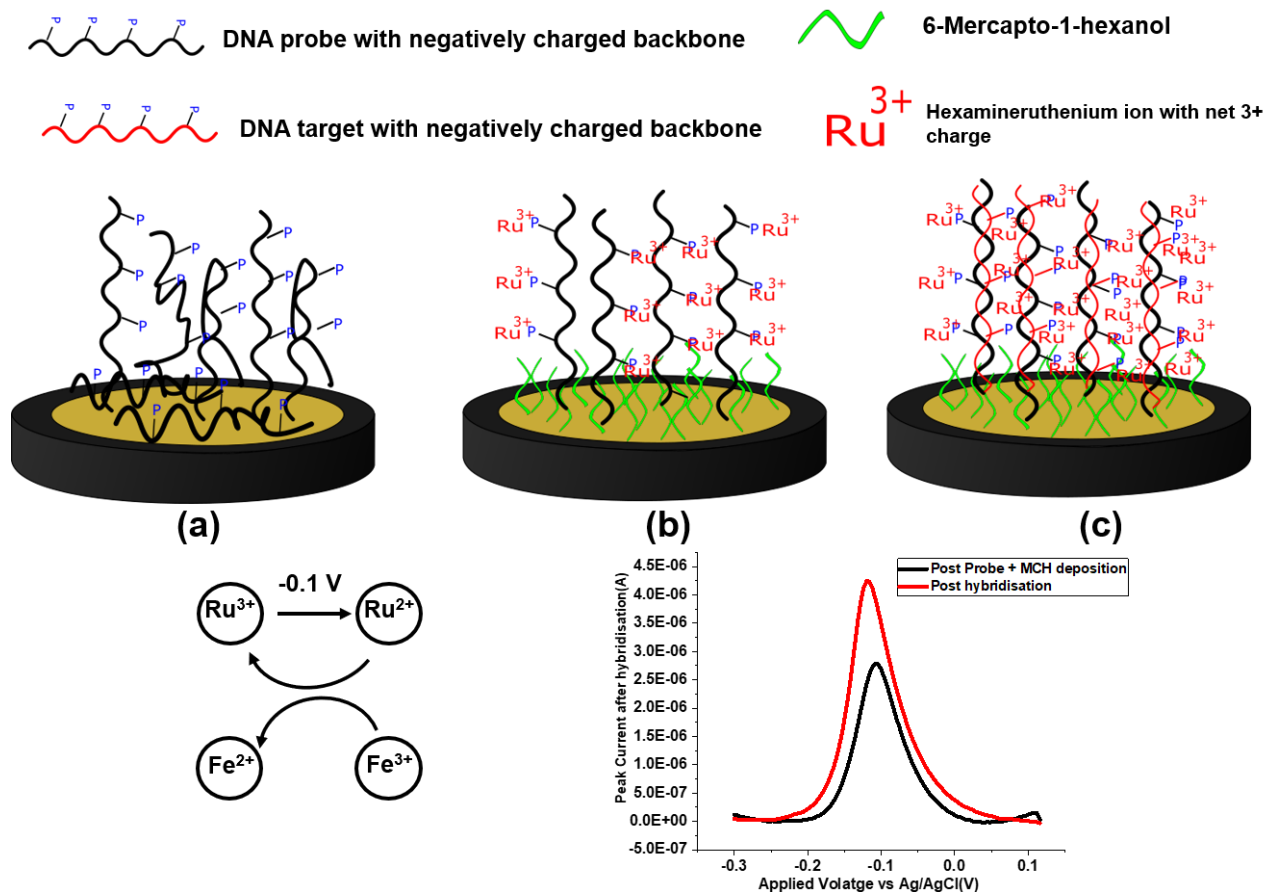


Figure 2.1. Sketch Map of Electrochemical DNA Sensing Strategy employing DNA probes. (a) DNA probes are immobilised on to a gold disk macroelectrode. **(b)** Mercapto-1-hexanol is used as a blocking agent to reduce non-specific adsorption of target DNA and to also align the probes in an upright and more accessible orientation for target strands. **(c)** Complementary target strand introduced. Differential pulse voltammetry (in 27 μM [Ru(NH₃)₆]³⁺, 2 mM [Fe(CN)₆]³⁻) was used to quantitate current generation at electrode surface before and after hybridisation with 1 μM complementary Target .

Hybridisation was measured as the signal change in RuHex/ FeCN solution before and after target introduction (Figure 2.1). Current is generated even when only probe DNA is

present because RuHex ions are attracted to the electrode surface via the negatively charged backbone of DNA. When 1 μM complementary target strands are introduced, there is even more negative charges at the electrode surface, leading to more RuHex ion attraction and an even larger current generation. When 1 μM non-complementary DNA was introduced, there was still an increase in current generation although not as much as with non-complementary DNA (45 % change in current for complementary target introduction vs 6.26 % for non-complementary) (Figure 2.2 c). This could be because even with MCH treatment, the monolayer formed is usually insufficient in covering the whole of the electrode surface [46], leading to non-specific adsorption of non-complementary target DNA onto the surface and attraction of Ru Hex ions to the surface. A key issue revealed with this system was the large pre-hybridisation background signal. In this case, when there is a variable probe density, the percentage change of the signal due to a specific target concentration varies significantly. This led to inconsistent signals, which made it difficult to obtain a limit-of-detection study for this assay. In order to eliminate this background signal, an assay using neutral peptide nucleic acid (PNA) probes was explored.

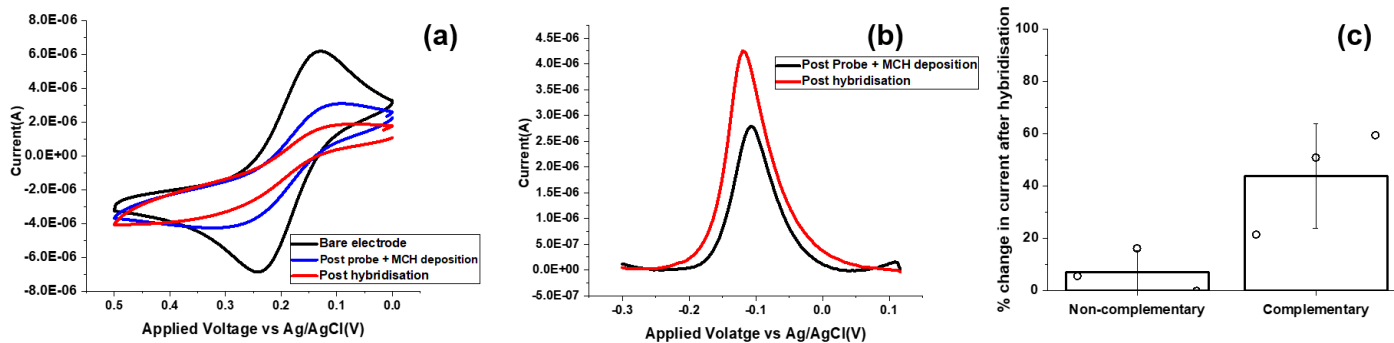


Figure 2.2. Characterisation of the modified electrode surface: a) cyclic voltammogram (in 2mM $[\text{Fe}(\text{CN})_6]^{4-}$) of gold electrode before probe deposition, after probe and MCH deposition and after target introduction b) Differential pulse voltammogram (in 27 μM $[\text{Ru}(\text{NH}_3)_6]^{3+}$ and 2 mM $[\text{Fe}(\text{CN})_6]^{3-}$) of gold electrode in the absence and presence of target DNA solution. c) Comparison of signal obtained before and after hybridisation in 27 μM $[\text{Ru}(\text{NH}_3)_6]^{3+}$, 2 mM $[\text{Fe}(\text{CN})_6]^{3-}$ for 1 μM Target samples (average taken from three trials, error bar represents standard deviation from the mean).

2.2.2 Implementation of in solution reporter system using PNA probes

In order to develop an assay with high sensitivity, specificity, and repeatability, we explored the use of peptide nucleic acid probes to eliminate background signals. PNA is a synthetic homolog of DNA or RNA in which the negatively charged phosphate backbone is substituted by a neutral pseudopeptide backbone. PNA can hybridise with complementary strands of DNA, and the resulting duplexes are more stable than DNA/DNA duplexes. This has been ascribed to the backbone of PNA being uncharged leading to less electrostatic repulsion in PNA/DNA duplexes compared to DNA/DNA duplexes[47].

The electrochemical detection strategy employed was as with the DNA probes. As the PNA probes have a neutral charge, it is expected that a reduced amount of RuHex ions

would be attracted to the electrode surface before hybridisation reducing the background current generated (Figure 2.3). Reduction of the background signal amplifies the signal changes obtained with the introduction of target strands. This reduces the risk of false negatives. Hybridization of probe PNA with target DNA leads to the attraction of RuHex ions to the electrode surface and a current is generated when the surface of the electrode is probed with a potential. (Figure 2.3 c)

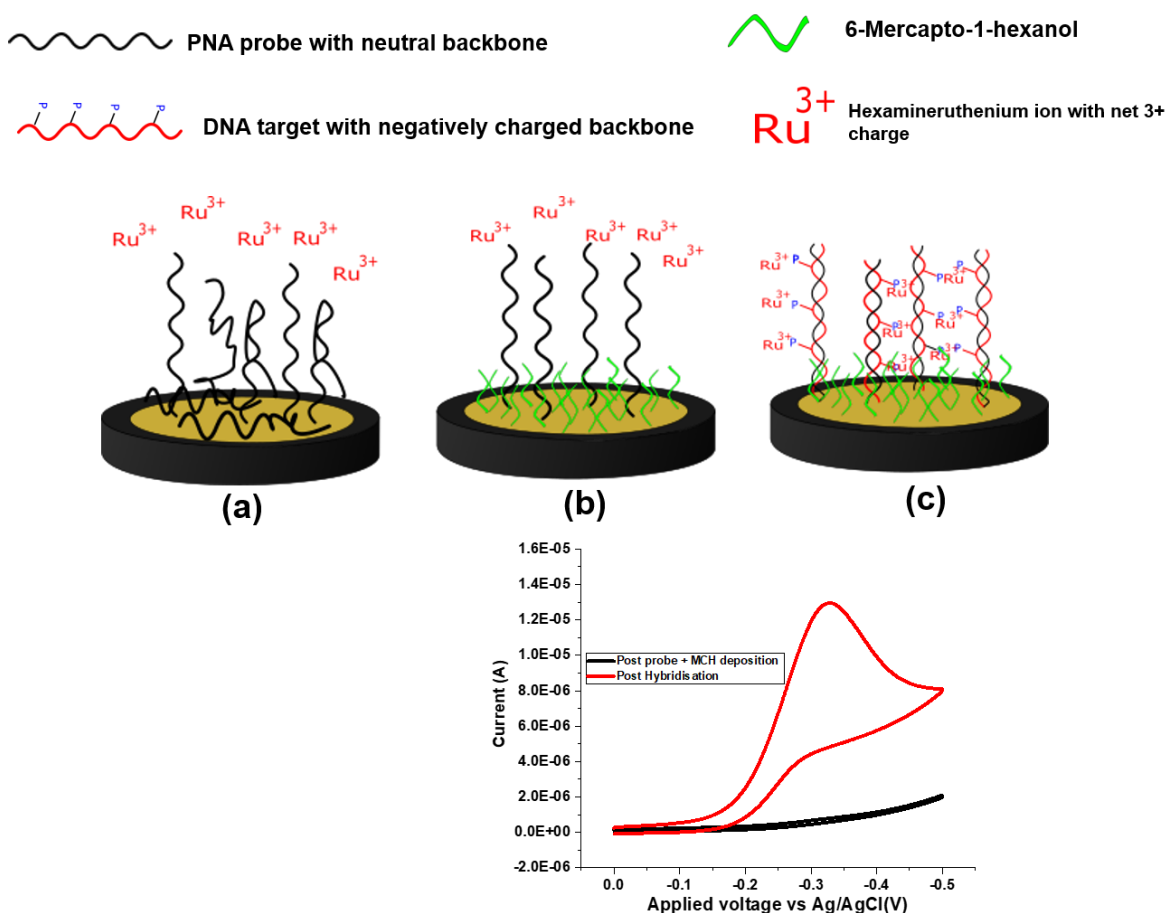


Figure 2.3. Sketch Map of Electrochemical DNA Sensing Strategy employing PNA probes. (a) PNA probes are immobilised on to a macro structured gold disk electrode. (b) Mercapto-1-hexanol is used as a blocking agent to reduce non-specific adsorption of DNA and to also align the probes in an upright and more accessible orientation for target strands. (c) Complementary target strand introduced. Cyclic voltammetry (in $27 \mu\text{M} [\text{Ru}(\text{NH}_3)_6]^{3+}$, $2 \text{mM} [\text{Fe}(\text{CN})_6]^{3-}$) was used to quantitate charge accumulation at electrode surface before and after hybridisation with $1 \mu\text{M}$ complementary Target introduction.

With this change in probe of the assay, a limit of detection (LOD) of 0.001 nM (Figure 2.4) was obtained. The LOD in this case was defined as the lowest Target concentration that resulted in a charge accumulation signal greater than the non-complementary (NC) signal. Defining the LOD as the lowest concentration at which the complementary signal is greater than the NC signal plus three times its standard deviation (i.e $Q_C + 1 \text{ SD} \geq Q_{NC} + 3 \text{ SD}$) still gives a LOD of 0.001 nM.

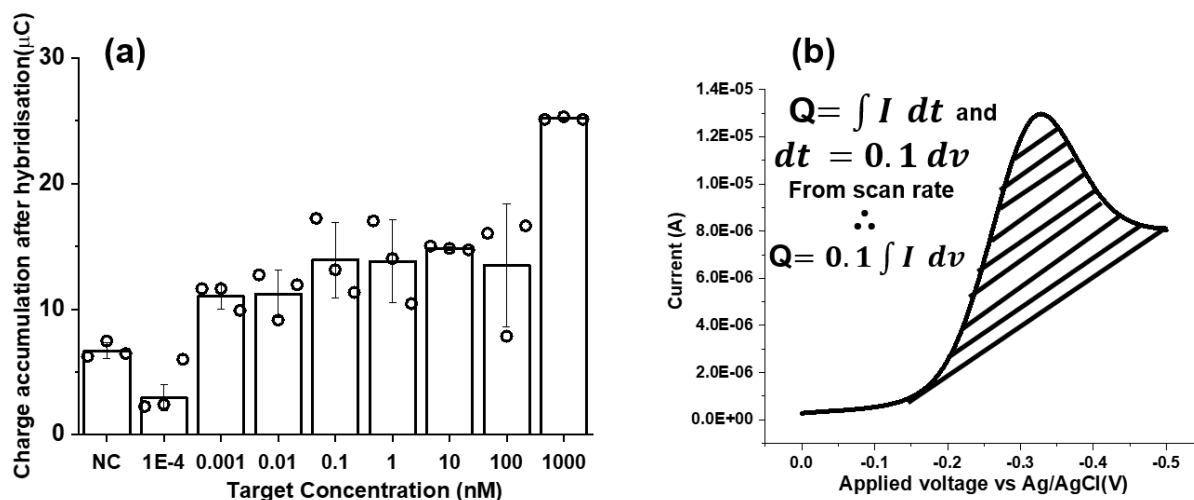


Figure 2.4. Detection limit of PNA assay. a) CV (in 27µM 27µM $[\text{Ru}(\text{NH}_3)_6]^{3+}$, 2 mM $[\text{Fe}(\text{CN})_6]^{3-}$) was used to quantitate the detection limit when complementary target solution was introduced. Non-complementary target was used to evaluate background levels and a detectible signal change down to 0.001 nM complementary target was attained. Averages taken from three trials, error bars represent standard deviation from the mean. b) Charge accumulation was calculated from integration of the area under the CV graph.

The LOD obtained was not in the usual log-linear form, and apart from the 1000 nM Target, all other complementary target concentration signals were around 12µC. This may be due to the hybridisation reaction at these lower concentrations being diffusion limited, leading to a similar rate of target capture at those concentration. This kind of mass

transport limitation happens when the hybridisation reactions occurring at the surface of a working electrode (WE) are faster than the target strands encountering the WE surface due to diffusion. Binding of the target strands to the probe strands creates a depletion area near the electrode surface, with target concentrations being lower here than in the bulk solution. This creates a diffusive flux where diffusion controls the rate of surface capture.[48] The much higher signal ($25\mu\text{C}$) obtained from the 1000 nM target may be due to the fact that at higher concentrations, hybridisation becomes a more reaction rate limited process than one controlled by diffusion or even convective transport.[49]

Even though there should have been no signal obtained, charge accumulation was still observed after hybridisation with non-complementary target. This is thought to be again because of the electrode surface not being completely covered after backfill with 1 hour, 1 mM MCH leading to non-specific adsorption of DNA targets to the gold electrode surface [1]. One way to bring down the non-complementary signal would be to backfill the electrodes a concentration of MCH greater than 1 mM and for a longer time. Another way would be to introduce simultaneous use of different kinds of blockers like polyethylene glycol (PEG) and bovine serum albumin (BSA). Both of these chemicals have been shown to reduce non-specific binding in sensor surfaces[50].

The LOD obtained from the electrochemical assay used for these experiments is within the range of what has been obtained before in literature. Lapierre et. al [2] performed electrochemical hybridisation with the RuHex/FiCN system using DNA probes on the same gold bulk electrodes used for our experiments and they were able to obtain a LOD in the nanomolar range. This shows that just by switching from DNA to PNA probes, we were able to improve this LOD from nanomolar range to picomolar range. Gasparac et.

al [51] improved upon Lapierre et. al's system by using nano-structured electrodes with DNA probes and they were able to detect signals in the picomolar range. Fang et al [52], using the previous nano-structured electrodes but switching to PNA probes, were able to detect signals in the femtomolar range.

To improve our system and to obtain an even lower LOD, we had planned to move onto nano-structured electrodes previously developed by Soleymani Group [53][54]. But due to the neutral backbone of PNA, which leads it to be hydrophobic[55], we began to experience solubility issues with the PNA. Thus, in order to achieve an even lower detection limit we sought to employ a programmable DNA strand displacement assay which introduced a built-in amplification into a system. Work done with this assay will be discussed in the next chapter.

2.3 Conclusion

In this chapter, in order to develop a rapid sample-to-answer time strategy for the detection of UTIs, a DNA probe RuHex/FiCN electro-catalytic reporter detection system was employed. Due to its negatively charged backbone, when DNA is used as the bio-recognition layer, the peak background signal is 2.78 μA , as such to enhance the system's limit-of detection, an assay based on the neutral bio-recognition layer, PNA was developed. PNA produced a lower background signal of 0.837 μA and a limit-of-detection of 0.001 nM. In order to enhance the LOD further, a new assay based on programmable strand displacement coupled with electrochemical read-out will be presented in the next chapter.

2.4 Experimental Section

Reagents

Acetonitrile (99.8 %), Potassium hexacyanoferrate(II) trihydrate (FoCN, 98.5-102.0%), Phosphate Buffer Solution (1.0 M, pH 7.4 (25°C)), Sodium chloride ($\geq 99.0\%$), Tris(2-carboxyethyl)phosphine hydrochloride (TCEP), Tris-EDTA buffer solution (TE, pH 8.0), 6-Mercapto-1-hexanol (MCH, 97%) and Hexaammineruthenium(III) chloride (RuHex, 98%) were purchased from Sigma-Aldrich (Oakville, Ontario). Potassium hexacyanoferrate (III) (FiCN, 60-100%) was purchased from Anachemia (Montreal, Canada). Sulfuric acid (H₂SO₄, 98%) was purchased from Caledon (Georgetown, Ontario). Ethanol (anhydrous) was purchased from Commercial Alcohols (Brampton, Ontario). All reagents were of analytical grade. Milli-Q grade water (18.2 M Ω) was used to prepare all solutions.

Electrode preparation

Assays were conducted using 2 mm diameter gold working electrodes purchased from CH Instruments. Electrodes were mechanically cleaned by first polishing them with 0.3 μm Alumina powder. They were then sonicated first in ethanol and then deionised (DI) water, each for 5 minutes. The same was repeated with 0.05 μm Alumina powder. The electrodes were electrochemically cleaned by scanning in 0.1 M Sulfuric acid for 80 cyclic voltammetry (CV) cycles at 0.1 V/s scan rate. The electrodes were rinsed with water and then dried in preparation for probe deposition.

Preparation of oligonucleotides. The following probe and target sequences were used in assays: seq. P1, DNA probe: 5' C6S-S-ATC TGC TCT GTG GTG TAG TT- 3'; seq. P1pna, peptide nucleic acid probe: C6SH-ATC TGC TCT GTG GTG TAG TT seq T1, complementary DNA target: 5' AAC TAC ACC ACA GAG CAG AT-3'; seq NC, non-

complementary DNA target: 5' TTT TTT TTT TTT TTT TTT TT-3'. DNA oligonucleotides were purchased from Integrated DNA Technologies and then resuspended in 1 x TE Buffer. PNA oligonucleotides were purchased from PNA Bio and then resuspended in 20 % acetonitrile. To reduce P1 and form a thiolated probe, the protocol in [56] was followed. To reduce any disulfide bonds that may form during the storage of PNA stock solution, 500 nM of PNA probe was mixed with 50 μ M TCEP and the reaction mixture left to sit at room temperature for 2 hours before deposition.

Modification of gold disk electrodes with DNA probes

A solution containing 1 μ M thiolated single-stranded P1, 25 mM phosphate buffer solution (PB), 25 mM NaCl, 100 mM MgCl₂ was prepared. 5 μ l of the probe solution was deposited on to the gold macroelectrodes and incubated overnight (16-18 hours) in a dark humidity chamber at room temperature. To prevent non-specific adsorption of DNA, 5 μ l of 1 mM MCH was deposited onto the electrodes for 1 hour and incubated in a dark humidity chamber at room temperature. Electrodes were rinsed in 25 mM NaCl, 25 mM Phosphate Buffer solution before electrochemical measurements.

Modification of gold disk electrodes with PNA probes

A 500 nM reduced PNA solution was prepared. The solution was then heated to 65 °C for 5 minutes and then cooled in an ice bath for 5 minutes. 20 μ l of the probe was deposited onto the electrode and the rest of the procedure was conducted as previously with the DNA probes.

Electrochemical Measurements

The electrodes were characterised by performing CV scans (0.05 V/s scan rate) in 2 mM FeCN, 25 mM NaCl, and 25 mM PB solution. Scans were conducted before and after probe deposition, after MCH deposition and after hybridisation with target strands. For DNA probe assay differential pulse voltammetry signals before and after hybridisation were collected with a scan rate of 0.1 V/s. For PNA probes, cyclic voltammetry was used. Signals were measured in solutions containing 27 μ M RuHex for DNA probes and 54 μ M RuHex for PNA probes, 2 mM FeCN, 25 mM NaCl, 25 mM PB. The baseline capacitive current was subtracted from the faradic current in the differential pulse voltammetry signal. For the DNA probe assay the % change in current due to hybridisation was calculated as follows: $\Delta I = (I_{af} - I_{bf}) / I_{bf} \times 100$ (af=after hybridisation, bf=before hybridisation). For the PNA probe assay, since there was no before hybridisation faradic peak, only the peak current after hybridisation was considered. The LOD of the PNA assay was defined as the lowest Target concentration that resulted in a charge accumulation signal greater than the non-complementary (NC) signal.

Hybridisation Protocol

For the DNA probe assays 5 μ l (20 μ l for PNA assays) of target solution was introduced onto the gold electrode surface. Target solutions consisted of 25 mM NaCl, 25 mM PB and 100 mM MgCl₂. Electrodes were incubated at 37 °C for 1 hour and then washed in 25 mM NaCl and 25 mM PB before electrochemical measurements were conducted.

Chapter 3

3.1 Introduction

Urinary Tract Infections (UTIs) have important health and economic consequences. They are the most common type of nosocomial infection [57]. The high prevalence of UTIs has led them to be one of the main contributors to antibiotic resistance[40] and in the US to have an associated societal cost of around US\$3.5 billion annually[58]. Currently, the most common practise to diagnose UTIs is a dipstick urinalysis and or a urine culture[9]. Although dipsticks are highly regarded as a rapid and in-expensive examination method[10], the procedures utility has been brought into question due to its lack of sensitivity[5]. While urine culture is considered the gold standard for UTI diagnosis[9], evaluation takes at least 24 hours. Matrix Assisted Laser Desorption/Ionization-Time of Flight (MALDI-TOF) can be used to lessen the time to pathogen identification to less than 5 hours and it only costs per sample half that of culture. But the initial price purchase of these instruments is over \$250 000 potentially restricting their use to high volume laboratories only [12]. As can be seen, current methods for UTI detection are either time consuming, or have low specificity, or are expensive and require operation by trained personnel.

As such, there is a great need for the development of an easy to use, rapid, sensitive and portable detection scheme for UTIs. To this end, due to their sensitivity, fast response and portability, electrochemical biosensors have emerged as an ideal contender for the evaluation of communicable diseases[28].In the previous chapter we presented a study

to develop an electrochemical sensor for nucleic acid detection of UTIs. Our chosen target was a 20-nucleotide long sequence analogous to a section of *E. coli* mRNA. *E. coli* is chosen as the analyte of interest because it is the cause for about 70% of UTIs [58]. In order to produce low background signals, the system consisted of the neutral bio-recognition layer PNA and a limit of detection (LOD) of 0.001 nM was obtained. This is less than the clinically relevant concentration for UTI detection. The most commonly reported UTI threshold is 10^5 cfu/ml [4] although some labs use 10^4 cfu/ml [2]. Using the generalisation of the molar concentration formula, this translates to about 0.1 or 0.01 fM respectively and assuming a conservative 100 mRNA copies per cfu, this means a clinically relevant concentration for our device would be about 1-10 fM.

In order to achieve this LOD we implemented a programmable strand displacement electrochemical assay with built-in amplification via target cycling, designed and validated using fluorescence by Li Group at Brock University. This assay is adapted from their protein responsive programmable DNA assembly presented in [59].

3.2 Results and discussion

The principle used in this assay is that of toehold-mediated strand displacement, which was first introduced and explored by Yurke *et al.* [60]. This work presented strand displacement as a means to animate DNA nanostructures, leading to the creation of the field now referred to as dynamic DNA nanotechnology. In particular, due to the ease with which nucleic based systems can be interfaced with biological DNA/RNA, dynamic DNA nanotechnology has seen the greatest amount of activity in research directed at medical diagnostics. As such a plethora of strand displacement systems have been proposed for

biosensing, yielding various detection limits from picomolar[61], femtomolar[62] to attomolar[63] sensitivity depending on the specific detection scheme.

In our assay (Figure 3.1), our Target strand, acting as the input to the system, binds to the L1T1RP duplex at the toehold (1). This releases the L1 strand creating the toehold (2). AP strand displaces RP strand using toehold (2). In the process, AP also displaces Target strand freeing it to take place in the reaction again as an input. It is in this manner that the Target strand is cycled, until the depletion of the L1T1RP duplex, creating built-in amplification into the system. This mechanism of using the same input strand to partake in multiple strand displacement cycles acting as a sort of catalyzer to the system was first described by Zhang *et al.*[64]. On a gold electrode the duplex probe CPD1 is immobilised. 6-mercapto-1-hexanol (MCH) is also immobilised for the purpose of reduction of non-specific adsorption of DNA onto the electrode surface[65]. Once the RP strand (which is modified with a methylene blue (MB) tag) is released, it binds to the CP strand at the electrode using toehold (3) displacing the protector strand D1. When RP binds to CP interrogation of the electrode surface with a potential leads MB to be reduced, producing a measurable signal. Before hybridisation with RP, there are no electroactive species near the electrode surface as such application of a potential yields no background current. Target strands were introduced to sensor surface in buffer solutions of 1 X Phosphate Buffered Saline (PBS) and 20 mM MgCl₂. Experiments were carried out in buffer in order to maximise signals under ideal conditions. This is in the hope that when actual urine samples are used, the inevitable dampening of the signal is not so great as to lead to total loss of signals.

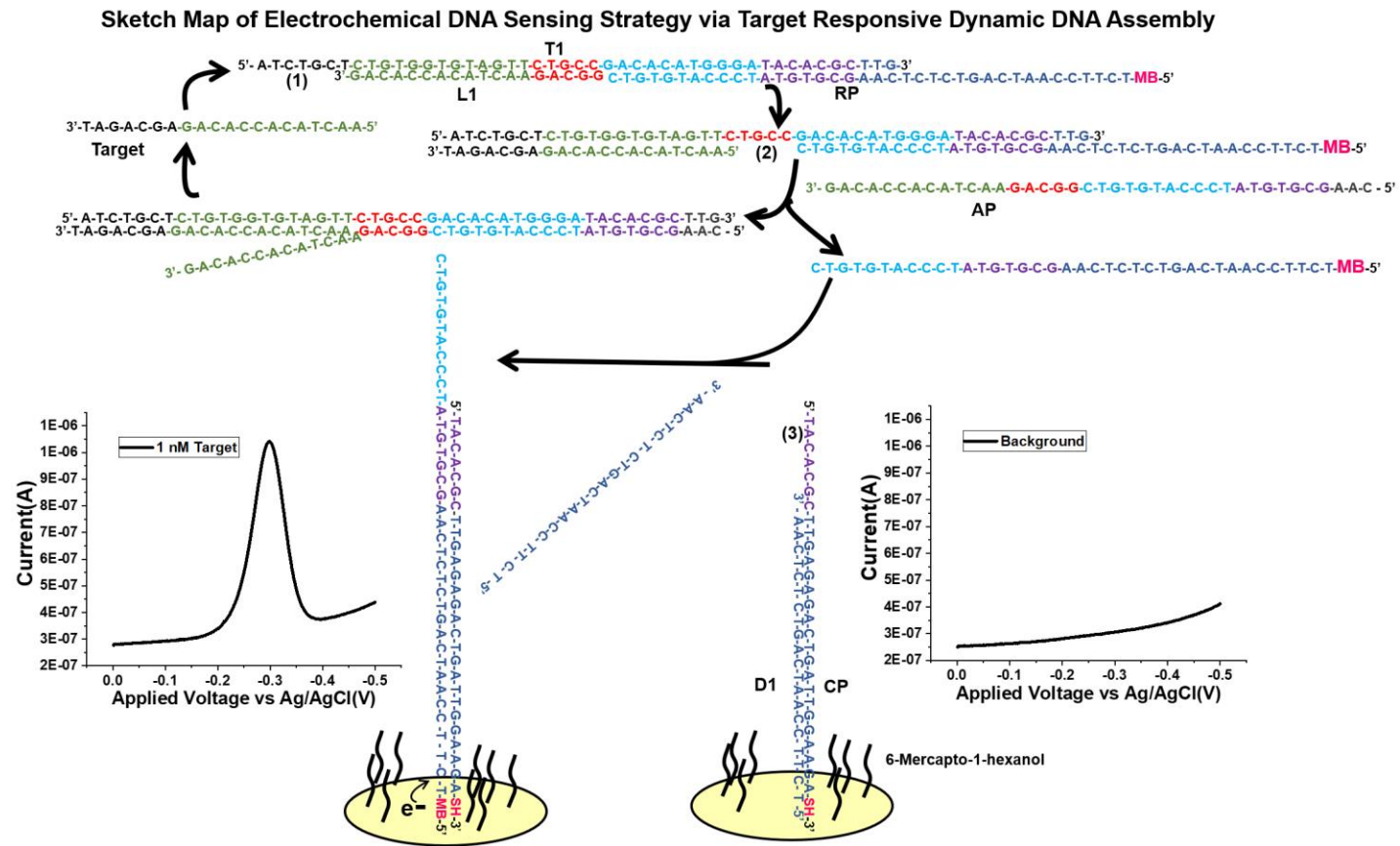


Figure 3.1 Sketch Map of strand displacement assay. Target strand binds to the L1T1RP duplex via toehold (1), and in the process displaces L1, creating toehold (2). AP strand binds to toehold (2) displacing MP tagged RP and Target strand. Target strand now free to cycle and bind to another L1T1RP duplex. This creates an in-built amplification into the system. Released RP binds to probe CP:D1, on electrode surface, via toehold (3) displacing protector strand D1. Application of potential to electrode now yields current as MB on electrode surface is reduced.

We characterised the electrode surface by running cyclic voltammetry scans in 2 mM $\text{Fe}(\text{CN})_6^{4-}$ (FoCN) solution (Figure 3.2 a). When the electrode surface is bare, the negatively charged FoCN ions can approach the electrode surface, such that when a potential is applied, the FoCN ions are oxidised and a current is generated. After deposition of the duplex probe DNA, there are more negative charges on the electrode surface, leading to the FoCN ions to be repelled and less oxidation to occur, hence less current is generated. This indicated that probe DNA strands were successfully deposited on the electrode surface.

After MCH deposition, an increase in current is observed, this is because when MCH is deposited it removes probes that have been weakly bound to the electrode surface, as well as helps the strongly attached probes to orient themselves in a vertical fashion[66]. This decreases the charge repulsion as well as the steric hindrance, allowing FoCN to have more access to the electrode surface.

Hybridisation was measured only as the signal obtained after target solution introduction (Figure 3.2). Before hybridisation, only the probe strand CP and its protector strand D1 are present in solution. Since in this case there are no electroactive species in the potential window scanned, the current generated is only due to the electrical double layer formed by ions in solution. This background current is a flat, slightly rising curve (Figure 3.2 b). After target solution introduction, the protector strand D1 is displaced by the MB tagged strand RP. As MB is electroactive in the potential window scanned, it is reduced and each MB molecule gains two electrons from the gold electrode ($\text{Methylene blue} + 2\text{e}^- + \text{H}^+ \rightarrow \text{Leuco-methylene blue}$ [67]). The current generated results in a peak around -0.3

V (Figure 3.2 b). Target solutions consisted of Target strand, L1T1RP and AP in Phosphate Buffered Saline (PBS) and 20 mM $MgCl_2$. In Figure 3.2 b after 1 nM of Target was introduced, a current (after baseline subtraction) of 0.696 μA was generated. In Figure 3.2 c a target solution with 0 nM Target strand was introduced to the electrode surface and a peak current of 0.298 μA was generated. Ideally, since there is no Target strand in this solution, there should be no displacement of the L1 strand and hence no toehold (2) created for the AP strand to displace MB tagged RP (Figure 3.1). The results show that RP is present at the electrode surface and is being reduced by the applied potential. This may be due to the annealing step not being 100% efficient leaving some free RP strands that can displace D1 and bind to CP. Another possibility is that the L1T1RP duplex has non-specifically adsorbed to the gold surface allowing for the reduction of MB. One way to reduce blank signals could be the simultaneous use of multiple blockers like polyethylene glycol (PEG) and bovine serum albumin (BSA). Both of these chemicals have been shown to reduce non-specific binding in sensor surfaces[50].

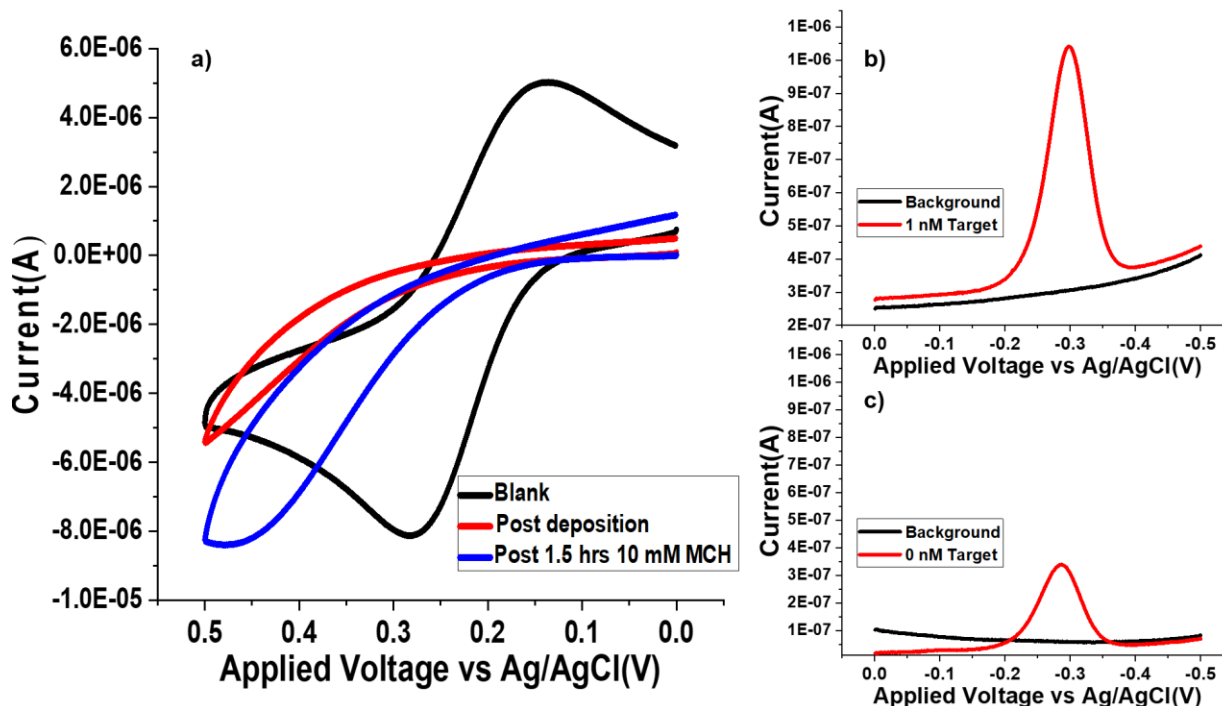


Figure 3.2. Characterisation of the modified electrode surface: a) cyclic voltammogram (in 2 mM [Fe(CN)₆]⁴⁻) of gold electrode before probe deposition, after probe deposition, and after MCH deposition b) Square wave voltammogram (in 25 mM NaCl/25 mM PBS) of gold electrode in the absence and presence of complementary target DNA solution c) Square wave voltammogram (in 25 mM NaCl/25 mM PBS) of gold electrode in absence and presence of 0 nM/“blank” target DNA solution. All plots use the convention cathodic (reductive) current positive.

In order to ascertain the optimal concentration of the intermediate L1T1RP, a simplified assay was employed (Figure 3.3 a). In this assay T1RP was reacted with AP to release RP. T1RP concentrations of 10, 50 and a 100 nM were tested. AP concentrations always equalled T1RP concentrations. Two sets of conditions were tested: one with AP present and one without AP present. This represented two scenarios. When AP is present, this is the maximum signal that can be obtained due to the full release of the RP strand. When

no AP strand is present, this is the noise signal: the signal produced even when no RP release has occurred. This noise signal is present due to that fact that the whole duplex T1RP can be bind to the duplex probe CPD1 without any strand displacement reaction occurring. This signal is also present because the annealing step of T1RP (and L1T1RP) is not 100% efficient and as such there is likely to be free RP in solution.

The maximum signal obtained to noise ratios from T1RP==AP==10,50 and 100 nM were 4.68,3.83 and 3.08 respectively, hence the optimal concentration for L1T1RP was found to be 10 nM from these experiments. However, in subsequent experiments 100 nM L1T1RP, AP was used. This was due to the fact that when the full assay was implemented (Target, L1T1RP, AP) 10 nM intermediates did not produce any signal (data not shown). This is thought to be because of the higher amount of negative charges in the target solution (with the introduction of L1 strand), which would make it more difficult to bring down the RP strand down to the electrode surface.

With this concentration of intermediates, a limit of detection (LOD) study was performed for the full assay (Figure 3.4). The signal obtained when there is no Target strand present is considered the blank or noise signal. The lowest Target concentration that resulted in a signal greater than the blank signal is considered the limit of detection. The LOD obtained for this assay was determined to be 10 nM as 10 nM Target yielded 0.1012 μA current while the blank signal was 0.029 μA .

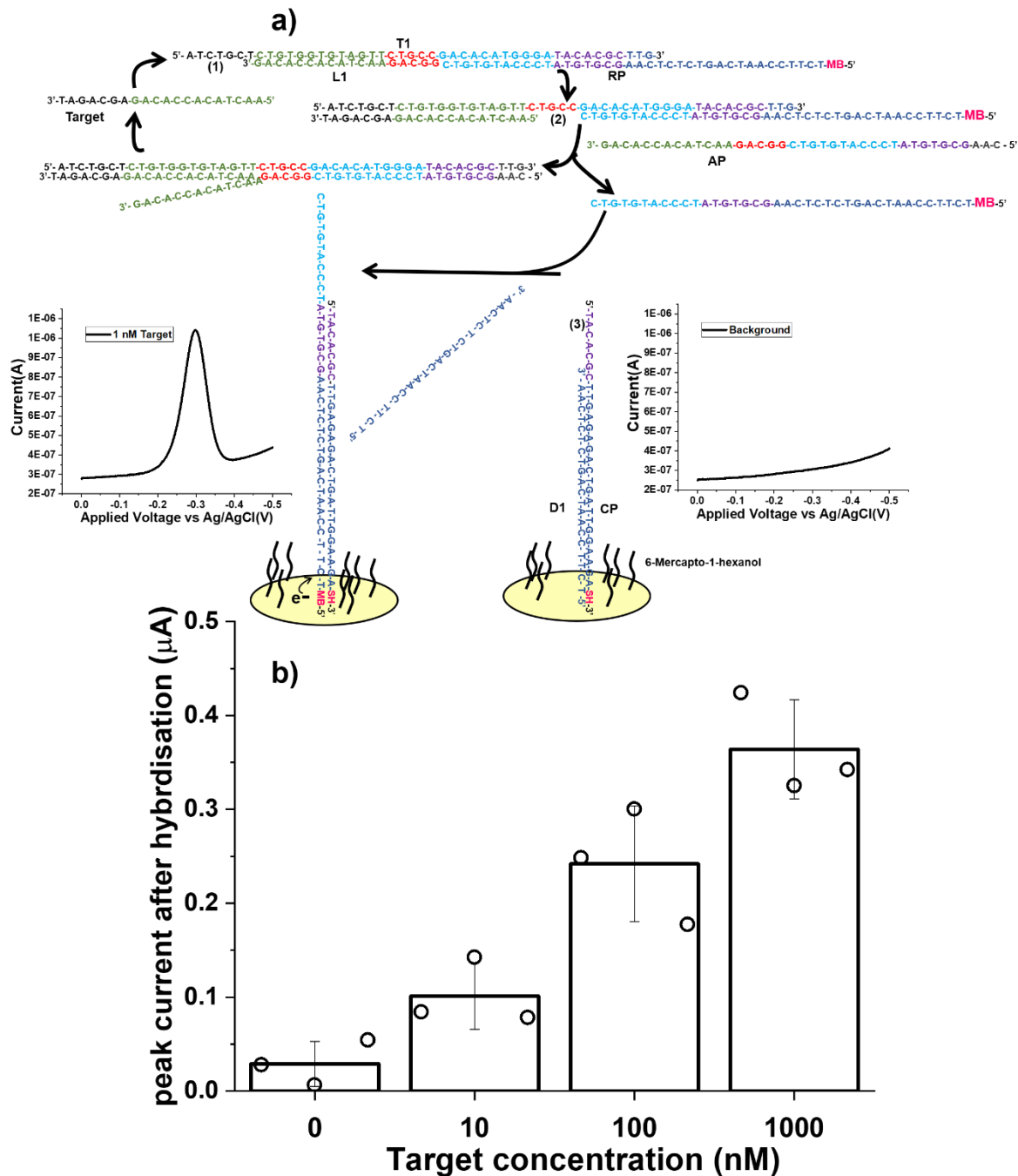


Figure 3.4. a) Schematic representation of full assay. b) The signal obtained after hybridisation with 10,100, 1000 nM Target strand. The blank signal (0 nM Target) is considered as the noise signal of the system. A detectable signal down to 10 nM complementary target was attained. Averages taken from three trials, the error bars represent standard deviation from the mean.

In another experiment (Figure 3.5), the LOD as defined previously, was found to be 0.5 nM. Although the signals obtained in this experiment were in the same order of magnitude as those obtained previously (100s of nAs), this experiment yielded much higher currents for lower concentrations. This is thought to be because although the deposition conditions were the same for the two experiments, they yielded different probe densities. The LOD for Figure 3.5 experiment was also defined theoretically using the Hubaux-Vos (HV) methodology, which can offer more consistent LODs[68]. Using this method, the LOD was found to be 0.26 nM and for the previous experiment the HV LOD was found to be 6.6 nM.

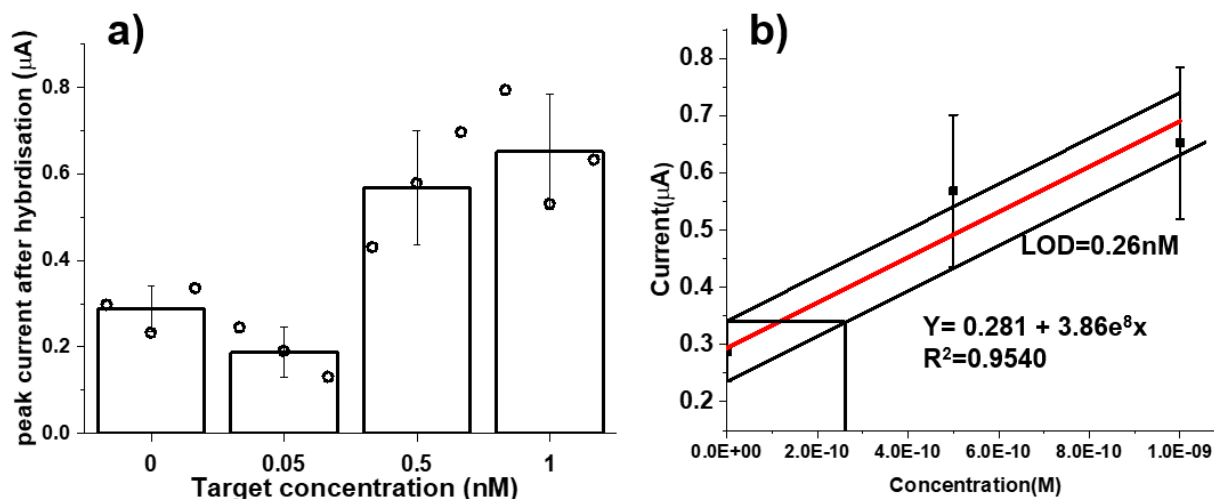


Figure 3.5. a) SWV responses of assay to different concentrations of target DNA at 0(Blank), 0.05 nM, 0.5 nM and 1 nM. A detectable signal down to 0.5 nM complementary target was attained. Averages taken from three trials; the error bars represent standard deviation from the mean. b) Determination of minimum detection limit using Hubaux-Vos methodology.

In order to ascertain whether or not the difference in current magnitude and LODs archived from the two previous experiments was due to different probe densities on electrode surfaces, an assessment of the post MCH FOCN curves (Figure 3.2a) of the electrodes was made. As previously discussed, assessment of FOCN CVs offers qualitative information on probe coverage of electrodes. The peak cathodic (reductive) and the peak anodic (oxidative) current were measured from all 24 electrodes used in the LOD experiments. It was found that the average peak cathodic and anodic currents were $1.99 \pm 0.84 \mu\text{A}$ and $8.34 \pm 0.97 \mu\text{A}$ respectively. Using the Grubbs outlier test there was found to be no significant outliers in the currents archived for the 0.05 significance level for both cathodic and anodic currents (Figure 3.6). The average currents achieved for the experiment where an LOD of 10 nM was obtained was $2.09 \pm 0.90 \mu\text{A}$ and $8.05 \pm 1.14 \mu\text{A}$ for the cathodic and anodic currents respectively. For the experiment where an LOD of 0.5 nM was achieved the currents were $1.90 \pm 0.80 \mu\text{A}$ and $8.63 \pm 0.68 \mu\text{A}$ for the cathodic and anodic currents respectively. For each experiment, the Grubbs test for outliers in each set of 12 electrodes showed no significant outliers for a significance level of 0.05 (data not shown). According to these data, there was not a significant difference between the probe densities between the two experiments yet they yielded LOD roughly two orders of magnitude apart. It is thought that due to the fact that in the experiment with the LOD of 10 nM, the samples were obtained from Li Group collaborators and were not independently quantified, the DNA samples received were of lower concentration than that which was labelled. In the experiment where 0.5 nM LOD was archived the DNA samples were quantified before use to ensure accurate concentrations.

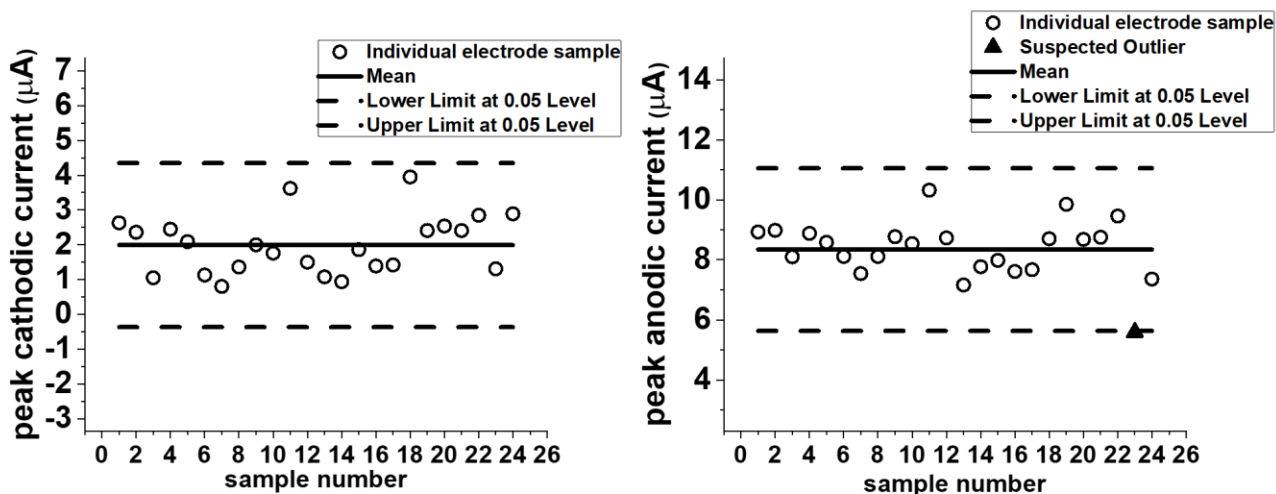


Figure 3.6 Grubbs outlier test for peak cathodic (left) and anodic (right) FOCN CV currents for all 24 electrodes used in the two LOD experiments. No significant outliers for peak currents were found.

In order to characterise the oligonucleotides involved in our assay a native polyacrylamide gel electrophoresis (PAGE) was ran. This technique is used to separate biological molecules according to their mobility in the gel. In this case the macromolecules are not denatured and are in their native state. An electric field is applied across the gel, evoking movement of negatively charged molecules away from the negative electrode and toward the positive electrode. The molecules move differently through the gel, according to their size. Smaller molecules move more easily through the pores of the gel, while the larger molecules have more difficulty. The gel is stained to allow visualisation of the separated molecules. Each distinct biomolecule appears as a distinct band on the gel.

In the gel in Figure 3.7 the single strands Target (1 µM), AP (1 µM), RP (1 µM), T1 (1 µM), and L1 (1 µM) were each loaded into lane 1,4,5,6,7 respectively. In order to be able to visualise it, the RP strand used in this experiment was not MB tagged. All other strands were the same as the ones used in electrochemical experiments. In lane 3, a solution of

Target (25 nM), AP (1 μ M), L1T1RP (1.2 μ M:1.1 μ M: 1 μ M) was loaded. This solution was allowed to incubate for 30 min at 37 °C prior to placement in the gel as this would permit the various strand displacement reactions to take place that would release the strand RP. In lane 2 a solution containing L1T1RP (1 μ M) and AP (1 μ M) was loaded. This was done in order to compare the results to when the Target strand is present. This solution of L1T1RP and AP was also allowed to incubate for 30 min at 37 °C prior to placement in the gel. Lane 8 consisted of a double stranded DNA ladder containing 11 DNA fragments in the range of 10 bp to 300 bp for use in tracking the movement of strands.

The results in lane 2 show that the complexes present are L1T1RP and AP. This is in line with what is expected, and although T1AP should be present (due to T1 being in excess of RP in the formation of L1T1RP and the formation of T1AP is more favourable to the formation of L1T1), it would have a concentration of around 100 nM and not be visible in the gel. L1 should also be present (L1 is in excess of both T1 and RP in the formation of L1T1RP), but as its concentration would be around 200 nM it is also not visible in the gel.

In lane 3, the complexes L1T1RP, T1AP, RP and AP are present, this is in line with what is expected since the target strand is present, the strand displacement of L1 should occur, leading to the displacement of RP by AP. L1T1RP is shown to still present in the solution. This may be due to the fact that the solution was hybridised for only 30 minutes and that is not enough time for the full release of RP via target cycling. L1 and Target strands should also be present in the gel but since they would be in low concentrations (not enough target cycling has occurred and displaced L1, and the target strand is only 25 nM) they are not visible in the gel. These results confirm the strand displacement of L1 (in

L1T1RP duplex) by the Target strand, as well as the strand displacement of RP and Target strand (in the TargetT1RP duplex) by AP.

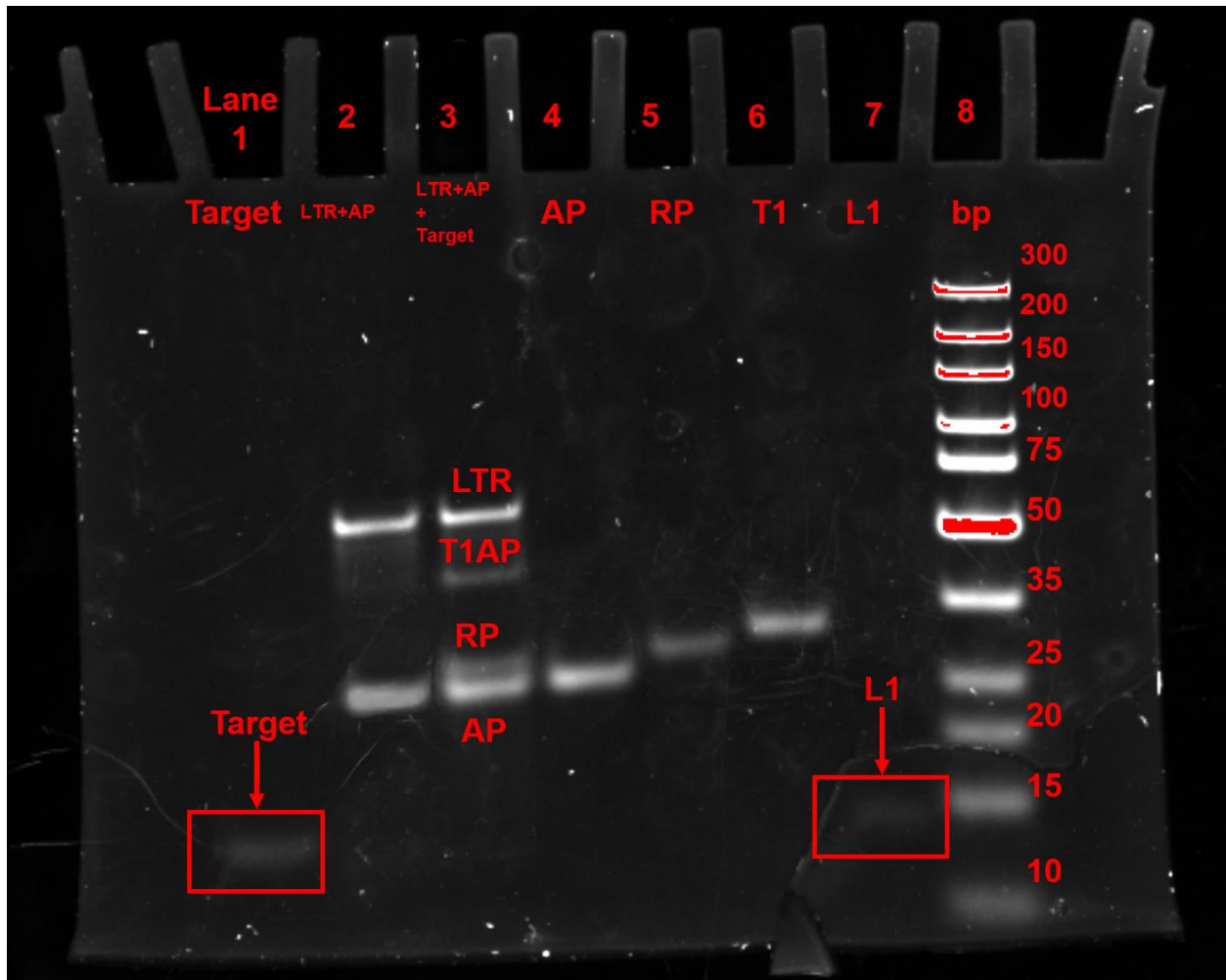


Figure 3.7 Characterisation of the oligonucleotides involved in the assay. Single stranded Target (1 μM), AP (1 μM), RP (1 μM), T1(1 μM), and L1(1 μM) strands were loaded into lanes 1,4,5,6,7 respectively. Lane 2 is from the analysis of a mixture containing L1T1RP and AP strands. Lane 3 is from the analysis of a mixture containing L1T1RP, AP and Target strands. A double stranded DNA Ladder was loaded into lane 8 to help in approximating the location of strands. Bands of the heavier complexes can be seen to have travelled shorter distances than lighter ones.

Comparing with literature, a similar system to the one presented here was found to have been employed by Shi et al.[69]. In their system, a three stranded DNA duplex probe was used to detect microRNA from cancer cells. The three-stranded duplex consisted of one long strand hybridised with two short strands. The miRNA-21 target binds to a terminal toehold on the probe, displacing one of the short strands through strand mediated displacement and in the process exposing a secondary toehold region. A methylene-blue (MB) – modified DNA strand uses this newly exposed toehold to bind to the probe, and in the process displaces both the miRNA-target and the other short strand. In this manner the miRNA-21 target is cyclically reused. This system was able to achieve a detection of miRNA-21 down to 1.4 fM. This was much lower than the detection limit for our assay which is 0.1 nM. With further optimisation of concentration of probe concentration (by testing a variety of probe concentrations against a constant concentration of target) and hybridisation time, a more comparable LOD might be archived with our assay. One difference between the two assays, is that in the assay employed by Shi et al., the target being detected is directly complementary to probe DNA. If another target was to be detected, there would be a need to change the probe and MB strand sequences. In our assay, the target instead induces the release of a strand RP that is complementary to the probe DNA CP. As such multiple types of targets could lead to the release of RP and there would be no need to change the probe DNA. This could be advantageous by helping to streamline the mass production of sensor chips.

3.3 Conclusion

In this chapter, to further pursue development of a detection strategy for UTIs, we implemented a novel programmable strand displacement electrochemical assay designed to have in built amplification via target cycling. We were able to achieve detection limits of 0.5 nM (0.26 nM in HV method). Further tuning of probe densities and hybridisation times could further enhance this LOD.

3.4 Experimental Section

Reagents. Potassium hexacyanoferrate(II) trihydrate (FoCN,98.5-102.0%), Phosphate Buffer Solution (PB Solution) (1.0 M, pH 7.4 (25°C)), Sodium chloride ($\geq 99.0\%$), Tris(2-carboxyethyl)phosphine hydrochloride(TCEP), Tris-EDTA buffer solution (TE, pH 8.0) , 6-Mercapto-1-hexanol (MCH,97%), Phosphate buffered saline (10x concentrate, BioPerformance Certified, suitable for cell culture) were purchased from Sigma-Aldrich (Oakville, Ontario). Sulfuric acid (H_2SO_4 , 98%) was purchased from Caledon (Georgetown, Ontario). Ethanol (anhydrous) was purchased from Commercial Alcohols (Brampton, Ontario). All reagents were of analytical grade. Milli-Q grade water (18.2 M Ω) was used to prepare all solutions.

Electrode preparation. Experiments were conducted using 2 mm diameter gold working electrodes purchased from CH Instruments. Electrodes were mechanical cleaned by first polishing them with 0.3 μm Alumina powder. They were then sonicated first in ethanol and then deionised (DI) water, each for 5 minutes. The same was repeated with 0.05 μm Alumina powder. The electrodes were electrochemically cleaned by scanning in 0.1 M Sulfuric acid for 80 cyclic voltammetry (CV) cycles at 0.1 V/s scan rate. The electrodes were rinsed with water and then dried in preparation for probe deposition.

Preparation of oligonucleotides. The following probe and target sequences were used in experiments: seq. L1: 5'-GGCAG AAC TAC ACC ACAG-3', seq. T1: 5'- ATC TGC T CTGT GGT GTA GTT CTGCC GAC ACA TGG GA TACA CGC TT G -3', seq. R: 5'- MB-TCT TCC AAT CA GTC TCT C AA GCG TGTA TC CCA TGT GTC -3', seq. AP: 5'- CAA GCG TGT A TC CCA TGT GTC GGCAG AAC TAC ACC ACA G-3', seq. CP: 5'- TACA CGC TT GAG AGA C TG ATT GGA AGA-SH-3' , seq. D1: 5'- TCT TCC AAT CAG TCTC TCAA-3',seq. Target: 5'-AAC TAC ACC ACA G A GCA GAT-3'. DNA oligonucleotides were purchased from Integrated DNA Technologies and then resuspended in 1 x TE Buffer. To form the duplex LTR the following annealing protocol was employed: 2.4 μM L1, 2.2 μM T1, 2 μM R oligonucleotides were mixed in a PCR tube. The LTR mixture was always annealed in a 1.2:1.1:1 ratio. The mixture was run in a Thermocycler with the following thermal profile: a) Heat to 90 °C and maintain temperature for 5 min b) Cool to 20 °C by decreasing the temperature by 5 °C increments and maintaining the temperature for 2 min. The annealing buffer composition was 1 X Phosphate Buffered Saline (PBS) and 20 mM MgCl_2 . The duplex probe CP/D1 was formed by mixing 15 μM of CP and 30 μM of D1. The CP/D1 mixture was always annealed in a 1:2 ratio. The annealing buffer was 25 mM phosphate buffer solution (PB), 25 mM NaCl, 100 mM MgCl_2 , and the same thermal profile as for annealing the LTR duplex was used. To reduce any disulfide bonds that may form during the storage of CP/D1 stock solution, 500 nM of the probe was mixed with 50 μM TCEP in 25 mM phosphate buffer solution (PB), 25 mM NaCl, 100 mM MgCl_2 and the reaction mixture left to sit at room temperature for 2 hours before deposition.

Modification of gold disk electrodes with DNA probes. 20 μl of the probe solution was deposited on to the gold macro electrodes and incubated overnight (16-18 hours) in a

dark humidity chamber at room temperature. To prevent non-specific adsorption of DNA, 10 μ l of 10 mM MCH was deposited onto the electrodes for 1.5 hours and incubated in a dark humidity chamber at room temperature. Electrodes were rinsed in 25 mM NaCl, 25 mM PB solution before electrochemical measurements.

Electrochemical Measurements. The electrodes were characterised by performing CV scans (0.05 V/s scan rate) in 2 mM FoCN, 25 mM NaCl, 25 mM PB solution. Scans were conducted before and after probe deposition and after MCH deposition. Square wave voltammetry signals before and after hybridisation were collected with amplitude of 0.025 V and frequency of 60 Hz. Signals were measured in solutions containing 25 mM NaCl and 25 mM PB solution. The baseline capacitive current was subtracted from the faradic current in the square wave voltammetry signal. Since there were no signals obtained for before hybridisation, only the peak current after hybridisation was considered. The detection limit for this assay was theoretically determined using Hubaux-Vos methodology.

Hybridisation Protocol. The intermediate strands LTR, AP and Target were mixed together in the ratio 100 nM:200 nM: x. The hybridisation solution was 1 X Phosphate Buffered Saline (PBS) and 20 mM MgCl₂. This reaction mixture was left too sit at room temperature for 15 minutes. 20 μ l of the reaction mixture was deposited onto the gold electrodes and incubated at 37 °C for 30 minutes and then washed in 25mM NaCl and 25 mM PB before electrochemical measurements were conducted.

Chapter 4

4.1 Thesis Findings and Contributions

This work demonstrated use of three different kinds of nucleic acid assays for the electrochemical detection of pathogenic genetic material.

In chapter 2 an electrocatalytic detection scheme using RuHex and FiCN [42] and DNA probes was used for the detection of mRNA *E.coli* targets. Electrodes deposited with 1 μ M probe targets showed a signal increase of 45 % with complementary targets compared to 6.26 % for non-complementary targets. A limit of detection study was not able to be done with this assay as this assay depended on signal changes for detection. Because probe densities varied from experiment to experiment this led to background currents being similarly varied and a consistent LOD was not achieved.

In order to reduce the background currents, PNA probes were implemented instead of DNA probes. PNA probes have a neutral backbone and as such do not attract any charged species to the surface. This meant for the RuHex/FiCN system, no electrocatalytic currents were observed before target introduction. It is in this manner a LOD series and a LOD of 0.001 nM was obtained. In theory no NC target signals should have been generated from the PNA assay since PNA is highly sensitive to target sequences and can even discern single nucleotide mismatch in targets [70] and non-specific adsorption is eliminated if electrodes are fully backfilled with MCH. It is suspected that the probe:MCH ratio of 1 μ M: 1 mM concentration was not optimal for these experiments hence the non-specific adsorption of non-complementary (NC) targets

yielded a signal of 6.68 μA . Further optimisation of probe:MCH ratios could bring down the NC signals, allowing for an even lower LOD to be obtained. Use of nano-structured electrodes to increase electroactive surface area [53] and sensitivity could also help this assay achieve a lower limit of detection. Due to difficulties with PNA solubility owing to it being slightly hydrophobic[55] further experiments with this assay were not performed.

In chapter 3, an electrochemical DNA biosensor based on enzyme-free target recycling amplification for the detection of mRNA *E.coli* targets was explored. The assay was designed and validated using fluorescence by Alex Wang of Li group at Brock University.

The assay consisted of a duplex probe CP:D1 self-assembled on an electrode surface. An intermediate three stranded duplex L1T1RP was used to mediate target capture and the release of a methylene blue modified strand which binds to the probe. The target strand binds to the duplex L1T1RP via a terminal toehold displacing the strand L1 and exposing a secondary toehold. This secondary toehold is used by the amplification strand AP which displaces the MB tagged RP as well as the target strand allowing the target strand to be reused. RP binds to the probe CP via another toehold mediated strand displacement.

The assay was optimised for electrochemical use by optimising the L1T1RP, AP concentrations and ratios using a simplified assay whereby T1RP was challenged with AP to see which concentration gave the best signal to background ratio. It was found that 10 nM of T1RP gave the best ratio at 4.68 but when these concentrations were used for the full assay no signals were obtained as such experiments proceeded with 100 nM L1T1RP intermediates.

In conclusion, this author's thesis findings have demonstrated three different systems for the detection of the same target. Switching the DNA probes to PNA, we were able to drive down the background current and achieve an LOD of 0.001 nM. In an effort to drive down this limit even further, a target recycling amplification assay was implemented. The LOD for this assay was found to be 0.5 nM, but further optimisation of probe concentrations and hybridisation times for this assay may yet still play a role in driving down the sensor's detection limit. The biggest contribution was the successful detection of targets using a novel electrochemical detection system that uses target cycling for in-built amplification.

4.2 Future Work

Immediate future work to be done involves improving the signal to noise ratio of the strand displacement assay introduced in this work. This can be achieved by bringing down the blank signal through increasing the concentration of magnesium ions in the annealing protocol in order to archive a greater efficiency in L1T1RP formation or increasing the incubation time of target solutions to increase complementary target signals. Decreasing the probe molar ratio from 1 μM probe:10 mM MCH may also help in increasing the hybridisation efficiency. It is possible that the current ratio has too many negative charges from the probe DNA backbone and not enough shielding by Magnesium ions repelling the RP strand from approaching the electrode surface. As such increase in Magnesium ions in the target solution may also help with increasing hybridisation efficiency. The limit of detection can be further improved by implementing nano-structured electrodes to increase electroactive surface area, as has been previously mentioned.

Distant future work would involve implementing this system using real mRNA targets in buffer, and eventually in real urine samples.

Chapter 5 Bibliography

- [1] C. M. Gonzalez and A. J. Schaeffer, "Treatment of urinary tract infection: what's old, what's new, and what works," *World J. Urol.*, vol. 17, no. 6, pp. 372–382, 1999.
- [2] C. M. Chu and J. L. Lowder, "Diagnosis and treatment of urinary tract infections across age groups," *Am. J. Obstet. Gynecol.*, vol. 219, no. 1, pp. 40–51, 2018.
- [3] L. Collins, "Diagnosis and management of a urinary tract infection," *Br. J. Nurs.*, vol. 28, no. 2, pp. 84–88, Jan. 2019.
- [4] G. Schmiemann, E. Kniehl, K. Gebhardt, M. M. Matejczyk, and E. Hummers-Pradier, "The diagnosis of urinary tract infection: a systematic review.," *Dtsch. Arztebl. Int.*, vol. 107, no. 21, pp. 361–7, May 2010.
- [5] R. Khasriya *et al.*, "The Inadequacy of Urinary Dipstick and Microscopy as Surrogate Markers of Urinary Tract Infection in Urological Outpatients With Lower Urinary Tract Symptoms Without Acute Frequency and Dysuria," *J. Urol.*, vol. 183, no. 5, pp. 1843–1847, May 2010.
- [6] S. Harini, A. Mambatta, V. Rashme, J. Kuppusamy, S. Menon, and J. Jayarajan, "Reliability of dipstick assay in predicting urinary tract infection," *J. Fam. Med. Prim. Care*, vol. 4, no. 2, p. 265, 2015.
- [7] A. S. Kupelian *et al.*, "Discrediting microscopic pyuria and leucocyte esterase as diagnostic surrogates for infection in patients with lower urinary tract symptoms:

- Results from a clinical and laboratory evaluation,” *BJU Int.*, vol. 112, no. 2, pp. 231–238, 2013.
- [8] K. C. Claeys, N. Blanco, D. J. Morgan, S. Leekha, and K. V. Sullivan, “Advances and Challenges in the Diagnosis and Treatment of Urinary Tract Infections: the Need for Diagnostic Stewardship,” *Curr. Infect. Dis. Rep.*, vol. 21, no. 4, p. 11, 2019.
- [9] Y. U. Budak, A. U. Karaca, M. Aydos, M. Bulut, and M. Polat, “Diagnostic accuracy of UriSed automated urine microscopic sediment analyzer and dipstick parameters in predicting urine culture test results,” *Biochem. Medica*, vol. 23, no. 2, pp. 211–217, 2013.
- [10] A. SK, N. T, R. N, and N. K, “Laboratory diagnosis of urinary tract infections using diagnostics tests in adult patients,” *Int. J. Res. Med. Sci.*, vol. 2, no. 2, p. 415, 2014.
- [11] G. Maugeri, I. Lychko, R. Sobral, and A. C. A. Roque, “Identification and Antibiotic-Susceptibility Profiling of Infectious Bacterial Agents: A Review of Current and Future Trends,” *Biotechnol. J.*, vol. 14, no. 1, 2019.
- [12] M. Davenport, K. E. Mach, L. M. D. Shortliffe, N. Banaei, T. H. Wang, and J. C. Liao, “New and developing diagnostic technologies for urinary tract infections,” *Nat. Rev. Urol.*, vol. 14, no. 5, pp. 298–310, 2017.
- [13] B. Foxman, “The epidemiology of urinary tract infection.,” *Nat. Rev. Urol.*, vol. 7, no. 12, pp. 653–60, 2010.

- [14] M. WJ, M. R, and R. S, “Validation of a decision aid to assist physicians in reducing unnecessary antibiotic drug use for acute cystitis,” *Arch. Intern. Med.*, vol. 167, no. 20, pp. 2201–2206, 2007.
- [15] S. D. Fihn, “Acute uncomplicated urinary tract infection in women,” *MeReC Bull.*, vol. 17, no. 3, pp. 18–20, 2006.
- [16] W. J. Mclsaac, D. E. Low, A. Biringer, N. Pimlott, M. Evans, and R. Glazier, “The Impact of Empirical Management of Acute Cystitis on Unnecessary Antibiotic Use,” *Arch. Intern. Med.*, vol. 162, no. 5, p. 600, Mar. 2002.
- [17] J. A. Karlowsky, D. J. Hoban, M. R. DeCorby, N. M. Laing, and G. G. Zhanel, “Fluoroquinolone-resistant urinary isolates of *Escherichia coli* from outpatients are frequently multidrug resistant: Results from the North American Urinary Tract Infection Collaborative Alliance-Quinolone Resistance Study,” *Antimicrob. Agents Chemother.*, vol. 50, no. 6, pp. 2251–2254, Jun. 2006.
- [18] M. C. O’Grady, L. Barry, G. D. Corcoran, C. Hooton, R. D. Sleator, and B. Lucey, “Empirical treatment of urinary tract infections: how rational are our guidelines?,” *J. Antimicrob. Chemother.*, vol. 74, no. 1, pp. 214–217, 2019.
- [19] A. Kothari and V. Sagar, “Antibiotic resistance in pathogens causing community-acquired urinary tract infections in India: a multicenter study.,” *J. Infect. Dev. Ctries.*, vol. 2, no. 5, pp. 354–358, 2008.
- [20] B. A. Rogers, “Antimicrobial Resistant *Escherichia coli* Clinical , Epidemiological and Molecular Characteristics in the Australian Region,” 2014.

- [21] A. L. Flores-Mireles, J. N. Walker, M. Caparon, and S. J. Hultgren, “Urinary tract infections: Epidemiology, mechanisms of infection and treatment options,” *Nat. Rev. Microbiol.*, vol. 13, no. 5, pp. 269–284, 2015.
- [22] A. R. Ronald *et al.*, “Urinary tract infection in adults: Research priorities and strategies,” *Int. J. Antimicrob. Agents*, vol. 17, no. 4, pp. 343–348, 2001.
- [23] D. R. Thévenot, K. Toth, R. A. Durst, and G. S. Wilson, “ELECTROCHEMICAL BIOSENSORS: RECOMMENDED DEFINITIONS AND CLASSIFICATION *,” *Anal. Lett.*, vol. 34, no. 5, pp. 635–659, Mar. 2001.
- [24] C. Ding, H. Li, K. Hu, and J. M. Lin, “Electrochemical immunoassay of hepatitis B surface antigen by the amplification of gold nanoparticles based on the nanoporous gold electrode,” *Talanta*, vol. 80, no. 3, pp. 1385–1391, 2010.
- [25] D. G. Rackus, M. H. Shamsi, and A. R. Wheeler, “Electrochemistry, biosensors and microfluidics: a convergence of fields,” *Chem. Soc. Rev.*, vol. 44, no. 15, pp. 5320–5340, 2015.
- [26] D. Grieshaber, R. MacKenzie, J. Vörös, and E. Reimhult, “Electrochemical Biosensors - Sensor Principles and Architectures,” *Sensors*, vol. 8, no. 3, pp. 1400–1458, Mar. 2008.
- [27] J. D. Watson and F. H. Crick, “Genetical implications of the structure of deoxyribonucleic acid,” *Nature*, vol. 171, no. 4361, pp. 964–967, 1953.
- [28] A. Liu *et al.*, “Development of electrochemical DNA biosensors,” *TrAC - Trends Anal. Chem.*, vol. 37, pp. 101–111, 2012.

- [29] F. Scholz, *Electroanalytical Methods: A guide to experiments and applications*. Springer Berlin Heidelberg, 2010.
- [30] M. D. Harris, S. Tombelli, G. Marazza, and A. P. F. Turner, *Affibodies as an alternative to antibodies in biosensors for cancer markers*. Woodhead Publishing, 2012.
- [31] J. M. Janda and S. L. Abbott, "16S rRNA gene sequencing for bacterial identification in the diagnostic laboratory: Pluses, perils, and pitfalls," *J. Clin. Microbiol.*, vol. 45, no. 9, pp. 2761–2764, 2007.
- [32] R. Mohan *et al.*, "Clinical validation of integrated nucleic acid and protein detection on an electrochemical biosensor array for urinary tract infection diagnosis," *PLoS One*, vol. 6, no. 10, p. e26846, 2011.
- [33] J. C. Liao *et al.*, "Development of an advanced electrochemical DNA biosensor for bacterial pathogen detection," *J. Mol. Diagnostics*, vol. 9, no. 2, pp. 158–168, 2007.
- [34] K. E. MacH *et al.*, "A biosensor platform for rapid antimicrobial susceptibility testing directly from clinical samples," *J. Urol.*, vol. 185, no. 1, pp. 148–153, 2011.
- [35] J. C. Liao *et al.*, "Use of electrochemical DNA biosensors for rapid molecular identification of uropathogens in clinical urine specimens," *J. Clin. Microbiol.*, vol. 44, no. 2, pp. 561–570, 2006.
- [36] "ID / AST UtiMax." [Online]. Available: <http://genefluidics.com/20151123/wp-content/uploads/2018/08/UtiMax.pdf>. [Accessed: 25-Mar-2019].

- [37] Y. Sun, C. Wang, H. Zhang, Y. Zhang, and G. Zhang, “A Non-Enzymatic and Label-Free Fluorescence Bioassay for Ultrasensitive Detection of PSA,” *Molecules*, vol. 24, no. 5, p. 831, 2019.
- [38] S. A. Al-Sayari *et al.*, “Fabrication of Highly Sensitive Non-Enzymatic Glucose Biosensor Based on ZnO Nanorods,” *Sci. Adv. Mater.*, vol. 3, no. 6, pp. 901–906, 2012.
- [39] N. J. Tarlton, C. Moritz, S. Adams-Sapper, and L. W. Riley, “Genotypic analysis of uropathogenic *Escherichia coli* to understand factors that impact the prevalence of β -lactam-resistant urinary tract infections in a community,” *J. Glob. Antimicrob. Resist.*, Mar. 2019.
- [40] C. Costelloe, C. Metcalfe, A. Lovering, D. Mant, and A. D. Hay, “Effect of antibiotic prescribing in primary care on antimicrobial resistance in individual patients: Systematic review and meta-analysis,” *BMJ*, vol. 340, no. 7756, p. 1120, 2010.
- [41] J. Wang, “Electrochemical nucleic acid biosensors,” *Anal. Chim. Acta*, vol. 469, no. 1, pp. 63–71, 2002.
- [42] M. A. Lapierre, M. O’Keefe, B. J. Taft, and S. O. Kelley, “Electrocatalytic Detection of Pathogenic DNA Sequences and Antibiotic Resistance Markers,” *Anal. Chem.*, vol. 75, no. 22, pp. 6327–6333, 2003.
- [43] L. Soleymani, Z. Fang, E. H. Sargent, and S. O. Kelley, “Programming the detection limits of biosensors through controlled nanostructuring,” *Nat. Nanotechnol.*, vol. 4, no. 12, pp. 844–848, 2009.

- [44] B. Lam *et al.*, “Solution-based circuits enable rapid and multiplexed pathogen detection,” *Nat. Commun.*, vol. 4, no. 1, pp. 1–8, 2013.
- [45] W. E. Stamm, “An Epidemic of Urinary Tract Infections?,” *N. Engl. J. Med.*, vol. 345, no. 14, pp. 1055–1057, Oct. 2001.
- [46] R. Lao *et al.*, “Electrochemical interrogation of DNA monolayers on gold surfaces,” *Anal. Chem.*, vol. 77, no. 19, pp. 6475–6480, 2005.
- [47] M. Egholm Buchardt, O., Christensen, L., Behrens, C., Freier, S. M., Driver, D. A., Berg, R. H., Kim, S. K., Nordén, B., and Nielsen, P. E., “PNA Hybridizes to Complementary Oligonucleotides Obeying the Watson-Crick Hydrogen-Bonding Rules,” *Nature*, vol. 365, no. October, p. 566–568., 1993.
- [48] J. Bishop, S. Blair, and A. Chagovetz, “Convective flow effects on DNA biosensors,” *Biosens. Bioelectron.*, vol. 22, no. 9–10, pp. 2192–2198, 2007.
- [49] J. H. S. Kim, A. Marafie, X. Y. Jia, J. V. Zoval, and M. J. Madou, “Characterization of DNA hybridization kinetics in a microfluidic flow channel,” *Sensors Actuators, B Chem.*, vol. 113, no. 1, pp. 281–289, 2006.
- [50] V. Gau, S. C. Ma, H. Wang, J. Tsukuda, J. Kibler, and D. A. Haake, “Electrochemical molecular analysis without nucleic acid amplification,” *Methods*, vol. 37, no. 1, pp. 73–83, 2005.
- [51] B. J. Taft, A. D. Lazareck, R. Gasparac, M. A. Lapierre-Devlin, S. O. Kelley, and J. M. Xu, “Ultrasensitive Electrocatalytic DNA Detection at Two- and Three-Dimensional Nanoelectrodes,” *J. Am. Chem. Soc.*, vol. 126, no. 39, pp. 12270–

- 12271, 2004.
- [52] Z. Fang and S. O. Kelley, "Direct electrocatalytic mRNA detection using PNA-nanowire sensors," *Anal. Chem.*, vol. 81, no. 2, pp. 612–617, 2009.
- [53] S. M. Woo, C. M. Gabardo, and L. Soleymani, "Prototyping of wrinkled nano-/microstructured electrodes for electrochemical DNA detection," *Anal. Chem.*, vol. 86, no. 24, pp. 12341–12347, 2014.
- [54] C. M. Gabardo, A. Hosseini, and L. Soleymani, "A New Wrinkle in Biosensors: Wrinkled electrodes could be a breakthrough for lab-on-A-chip devices," *IEEE Nanotechnol. Mag.*, vol. 10, no. 2, pp. 6–18, 2016.
- [55] S. Sen and L. Nilsson, "Molecular dynamics of duplex systems involving PNA: Structural and dynamical consequences of the nucleic acid backbone," *J. Am. Chem. Soc.*, vol. 120, no. 4, pp. 619–631, 1998.
- [56] B. Fung, "A STUDY OF POROUS ELECTRODES FOR DNA ELECTROCHEMICAL DETECTION," McMaster University, 2016.
- [57] F. B., "Epidemiology of urinary tract infections: Incidence, morbidity, and economic costs," *Disease-a-Month*, vol. 49, no. 2, pp. 53–70, 2003.
- [58] A. L. Flores-mireles, J. N. Walker, M. Caparon, and S. J. Hultgren, "Urinary tract infections: epidemiology, mechanisms of infection and treatment options," *Nat. Rev. Microbiol.*, vol. 13, no. 5, pp. 269–284, 2016.
- [59] F. Li, Y. Lin, and X. C. Le, "Binding-induced formation of DNA three-way junctions and its application to protein detection and DNA strand displacement," *Anal.*

- Chem.*, vol. 85, no. 22, pp. 10835–10841, 2013.
- [60] A. P. Mills, F. C. Simmel, A. J. Turberfield, J. L. Neumann, and B. Yurke, “A DNA-fuelled molecular machine made of DNA,” *Nature*, vol. 406, no. 6796, pp. 605–608, 2002.
- [61] H. G. Chen *et al.*, “Fluorometric detection of mutant DNA oligonucleotide based on toehold strand displacement-driving target recycling strategy and exonuclease III-assisted suppression,” *Biosens. Bioelectron.*, vol. 77, pp. 40–45, 2016.
- [62] F. Yang *et al.*, “Toehold enabling stem-loop inspired hemiduplex probe with enhanced sensitivity and sequence-specific detection of tumor DNA in serum,” *Biosens. Bioelectron.*, vol. 82, pp. 32–39, 2016.
- [63] H. Ravan, M. Amandadi, and S. Esmaeili-Mahani, “DNA Domino-Based Nanoscale Logic Circuit: A Versatile Strategy for Ultrasensitive Multiplexed Analysis of Nucleic Acids,” *Anal. Chem.*, vol. 89, no. 11, pp. 6021–6028, 2017.
- [64] D. Y. Zhang and G. Seelig, “Dynamic DNA nanotechnology using strand-displacement reactions,” *Nat. Chem.*, vol. 3, no. 2, pp. 103–113, 2011.
- [65] A. Meunier, M. Steichen, C. Buess-Herman, A. De Rache, T. Doneux, and E. Triffaux, “Optimization of the Probe Coverage in DNA Biosensors by a One-Step Coadsorption Procedure,” *ChemElectroChem*, vol. 1, no. 1, pp. 147–157, 2013.
- [66] S. D. Keighley, P. Li, P. Estrela, and P. Migliorato, “Optimization of DNA immobilization on gold electrodes for label-free detection by electrochemical impedance spectroscopy,” *Biosens. Bioelectron.*, vol. 23, no. 8, pp. 1291–1297,

2008.

- [67] E. Papadopoulou, N. Gale, J. F. Thompson, T. A. Fleming, T. Brown, and P. N. Bartlett, “Specifically horizontally tethered DNA probes on Au surfaces allow labelled and label-free DNA detection using SERS and electrochemically driven melting,” *Chem. Sci.*, vol. 7, no. 1, pp. 386–393, 2016.
- [68] J. Schibler, D. Moore, B. De Borba, and D. Corporation, “Setting Meaningful Detection and Quantitation Limits for Chromatography Methods Detection and Quantification Limits,” *Dionex Corp.*, no. June, pp. 1–4, 2007.
- [69] K. Shi, B. Dou, C. Yang, Y. Chai, R. Yuan, and Y. Xiang, “DNA-Fueled Molecular Machine Enables Enzyme-Free Target Recycling Amplification for Electronic Detection of MicroRNA from Cancer Cells with Highly Minimized Background Noise,” *Anal. Chem.*, vol. 87, no. 16, pp. 8578–8583, 2015.
- [70] K. Hashimoto and Y. Ishimori, “Preliminary evaluation of electrochemical PNA array for detection of single base mismatch mutations,” *Lab Chip*, vol. 1, no. 1, pp. 61–63, 2001.